Trace Elements in Marine Sediments from the Oxfordian (Late Jurassic): Implications for Seawater Chemistry, Erosional Processes, Changes in Oceanic Circulation and More

Barbara Müller*

Geological Institute, Swiss Federal Institute of Technology, 8092 Zürich, Switzerland

Abstract: The Oxfordian, first stage of the late Jurassic, is remarkably variable in terms of deposited sediments, geochemical tracers, and climate. The climate changed during the Middle Oxfordian from humid to arid with a temperature rise of more than five degrees. During this time, the $\partial^{13}C$ reached maximum values. The positive excursion in $\partial^{13}C$ of carbonates from the Oxfordian (with an amplitude of more than 1‰) was reproduced in hemipelagic sections from southeastern France. Analysis of major and trace elements of these carbonates were carried out by LA-ICP-MS in order to verify their application as palaeoproxies in conjunction with the changes mentioned in climate. As a novel approach 36 elements were measured with regard to establish a complete and comprehensive analysis of the geochemical situation. Concentration peaks of P, Sr, Mn, Fe, Ba point to a more oligotrophic setting within the lower part of the sediment profile from southeastern France. Conversely, the positive $\partial^{13}C$ excursion with $\partial^{13}C$ values rising from 2 to 3 ‰ within the uppermost part of the profile coincide with more elevated concentrations of V, Fe, Mn, U arguing for an ocean-wide anoxia (Oceanic Anoxic Events OAE). High detrital input during this arid period is recorded by enhanced concentrations of elements like Ti, Mn, Fe, Zr, Nb and W. This correlation of the $\partial^{13}C$ excursion with trends in Ti, Nb, W as well as Mn and Fe contents reflects changes in the Oxfordian palaeooceanography and climate. During the late Oxfordian the environmental prerequisites were controlled by warm and arid conditions and an increased metal flux from the continent due to the intensified chemical and physical weathering, erosion of rocks, as well as aeolian and fluvial transport to the oceans.

Keywords: Oxfordian, carbon isotopes, trace elements, palaeoproxies, climate change, ocean-wide anoxia.

INTRODUCTION

The Oxfordian (~ 160 to 155 m.y. BP, the first stage of the Late Jurassic) was a time of widespread, globally near synchronous change in the marine (carbonate) sedimentation pattern [see 1 and references therein]. One of the most striking features of this time interval is the switch from dark and clayey or siliceous carbonate-poor sediments to light grey, carbonate-rich deposits. This peculiar switch, which is very distinct and obvious in the field, defines the boundary between "brown" and "white" Jurassic - reflecting the fundamental global changes the world was undergoing at that time [1]. The sudden and widespread changes in the marine carbonate sedimentation pattern, therefore, must be part of a response of the ocean-atmosphere-solid earth system to internal or external forces [see 1 and references therein]. In the European Tethys province, the late Callovian and Early Oxfordian are distinguished by reduced carbonate deposition: sediments are either absent, condensed and iron-rich or were built as thick, organic carbon-rich shaly (e.g. "Terres Noires") or siliceous deposits (e.g. radiolarites). Later, in the middle to late Oxfordian, a change to widespread carbonate sedimentation occurred. This well documented change in sedimentation pattern seems to correlate with a positive anomaly in both marine and terrestrial carbon-isotope records of the middle Oxfordian [1].

Moreover, the climate was also undergoing major changes during the Oxfordian: the Late Callovian-Early Oxfordian was characterized as a cold and humid period and was replaced by a considerably warmer and more arid climate in the middle-late Oxfordian. This change led to increased metal flux from the continent due to the intensified chemical weathering due to the higher temperatures and enhanced erosion rates [1, 2 and references therein]. Along with the ongoing opening of the Atlantic and the Tethys, the Late Jurassic long-term sea-level rise led to a reorganization of ocean currents in the Tethys-Atlantic system during the Oxfordian [1].

Carbon-isotope records of marine carbonate are a useful proxy of the carbon cycle. In Louis-Schmid *et al*. [1] the authors investigated detailed C-isotope records of the early to middle Oxfordian from France and Switzerland. They studied the relationship between C-isotope evolution, facies changes, carbon cycling and sea level, followed by a discussion of mechanisms responsible for the mid-Oxfordian positive C-isotope excursion.

The study [1] was centered on the northern margin of the Tethys. This region was once close to the confluence of the opening Atlantic and Tethys oceans and, therefore, it seems clear that it responded sensitively to changes in global ocean circulation patterns. The area studied is comprised of

*Address correspondence to this author at the EAWAG, Swiss Federal Institute of Aquatic Science and Technology, 8600 Dübendorf, Switzerland; Tel: +41(0) 79 656 70 54; E-mail: barbara.mueller@eawag.ch

1874-2629/12

hemipelagic to pelagic environments, which are supposed to be influenced to a minor extent only by land areas. Therefore these areas are still shallow enough to record the changes in sea level and are also distinguished by high sedimentation rates. Two composite sections were measured for the above mentioned study: One from southeastern France (Trescléoux/Oze) and a second from the Swiss Jura (Liesberg).

The lower part in Trescléoux and Oze (southeastern France) belongs to the "Terre Noires" facies and consists of gray to black marls with layers of carbonate nodules. The upper part belongs to the "Argovien" facies (marls with marly limestones). Both sites were sampled at a 1m resolution at Trescléoux; 112 samples out of 102 m at Oze.

However all the prior studies [1-3] lack the information about trace element contents in these sediments. For to this reason the following study was accomplished. The distribution of trace elements in marine sediments provides the necessary information about the seawater chemistry in the past, about weathering and erosion processes and about sudden changes in oceanic circulation as well as about biogeochemical cycles [4, 8-10, 18]. Moreover, marine sediments provide important information on past oceanographic and climatic changes, such as fluctuations in biological productivity, redox state of bottom water, seawater and sediments, tectonic activity, wind strength and volcanic, hydrothermal, hydrogenous, aeolian and fluvial sources [4]. As the changes related to these processes cannot be determined directly, geochemical proxies of climatic and palaeoenvironmental constraints have been developed during the last several decades (e.g. [5-20]).

Bruland [21] provided a detailed and comprehensive review on concentration-depth profiles of trace elements involved in biogeochemical cycles of metal uptake, recycling and particulate deposition. In his study he also addressed the distribution of elements which are either conservative in oxygenated water, are removed from solution by adsorptive scavenging, or are removed by precipitation under anoxic conditions. The most important of his findings was that most trace metals are largely involved in bio-cycling processes In Craig and Miller [22] a comprehensive overview about metal ions and their organometallic compounds in sea water and sediments as well as the related biogeochemical cycles is provided.

In Brumsack and Rinna *et al*. [18, 23] the authors stated that organic-rich sediments are usually enriched in several redox-sensitive elements like Mo, V, Cu, Zn or U and stable sulfide-forming trace elements and that they form an important sink in global trace metal cycles. These enrichments must bear a relation to their abundance in seawater (e.g. [24]).

According to Calvert and Pedersen [8] the concentrations of trace and minor elements in marine sediments reflect the range of chemical, oceanographic and sedimentary controls on their supply to, their distribution in and their removal from the ocean. Such controls include the composition of sedimentary detritus delivered to the ocean, the partitioning of individual elements between solid and solution phases, the biogeochemical cycling of the elements in the ocean, the manner in which they are delivered to the sea floor, and the post-depositional conditions in bottom sediments that may lead to diagenetic element recycling or precipitation. As shown in various studies, minor and trace elements behave differently under oxic and anoxic marine conditions and they naturally fall into two categories: 1) Elements whose valency can vary as a function of the actual redox potential: Mn, Cr, Mo, Re, U, V. These elements occur as highly soluble anionic species in oxic waters but are reduced to insoluble species of lower valency under anoxic conditions [6, 11]. 2) Elements like Cu, Ni, Zn and Cd are usually removed from solution in the presence of H_2S [8]. Pyrite, the most common sulfide in marine sediments prevalently contains Mn, Co, Ni and Cu as trace elements. Elements as mentioned above are, therefore, of prime use as palaeoproxies. A palaeoproxy record of the climate contains a climatic signal, which can be used to infer qualitative and quantitative information about the past on inter-annual to multi-millenial timescales.

Initially, trace and minor elements are supplied to the site of deposition from terrestrial sources *via* rivers or the atmosphere, from biological activity within the ocean and from ocean bottom waters. The latter group is commonly called the authigenic fraction of trace and minor elements. Elemental palaeoproxies like Si, Fe, K, Mg, Ti and Co are of detrital origin, whereas elements like Ba, P, Zn are attributed to be nutrient-related (e.g. [16, 18]). Enhanced concentrations of Zr and Nb seem to be of volcanogenic origin [21, 25, 26]. High concentrations of Ag and Zn in marine sediments are also assigned to hydrothermal input [4, 18, 27, 28]. Ti, Zr and Nb are often concentrated in heavy-metal mineral associations, whereas Ca and Sr reflect the occurrence of carbonate [29].

Biogenic remnants in marine sediments contain Si, Al, Fe, K, Ca, Mg, Na, Ti, Mn and P. Zn, Ni, Cd, Cu and Se are highly enriched in plankton [21]. V, Mn, Fe, Co, Ni, Cu and Zn play an important role in metal-requiring and metal-activated enzyme systems and protein metabolism in phytoplankton [21] as well as in ancient and in recent bacteria [30].

In Kuhn *et al*. [31] it is reported that the enrichments of Mn and Fe in carbonates of Valanginian (Cretaceous) age deposited in the Tethys and Atlantic Oceans, which also show a positive $\partial^{13}C$ excursion. The correlation of the $\partial^{13}C$ excursion with trends in Mn and Fe contents seems to reflect changes in Valanginian palaeooceanography and climate. High concentrations of Mn of the early Toarcian, Late Jurassic, Aptian, Albian, Cenomanian/Turonian boundary and Miocene seem to be correlated with ocean-wide anoxia (Oceanic Anoxic Events OAE) and/or changes in the carbon cycle as expressed by positive $\partial^{13}C$ excursions [31, 32]. In Bodin *et al*. [33] an enrichment of redox-sensitive trace elements (U, V, Mo, and As) associated with the late Hauterivian (Early Cretaceous) Faraoni oceanic anoxic event was found. There is a certain debate over the latter interrelation. On the contrary, no evidence of an OAE from transects in the western Tethys from the Valaginian period of time (Early Cretaceous) was found [34]. The concentrations of the redox-sensitive elements like U, V, Co and Mo were not as enriched as expected for reductive bottom-water conditions within the respective transects. The enhanced concentration of Mn was attributed to an increase in continental influx, combined with higher Mn redox-recycling.

They conclude that anoxic events were rather limited to marginal seas.

The goals in this paper are to present the chemical analyses and the determination of 36 trace elements in the Oxfordian marine sediments from two localities in southern France. The correlation of these trace element contents with the two positive $\partial^{13}C$ excursions and their use as palaeoproxies will be discussed. The unambiguous, broad and unique correlation of these trace elements to oceanographic and climatic changes - such as fluctuations in biological productivity, redox state of bottom water, seawater and sediments, tectonic activity, wind strength as well as volcanic, hydrothermal, hydrogenous, aeolian and fluvial sources - will be illustrated.

STUDY SITE AND SAMPLE MATERIAL

The studied composite section, exposed near Serres (SE-France), was deposited in the Tethyan Subalpine basin, a deep epeiric basin influenced by tectonics related to the opening of the Alpine Tethys and the Atlantic (Fig. **1**).

Two separate sections were analyzed, outcropping at a distance of about 500 meters from each other. Sampling was performed at 1m-resolution. The lower part is exposed on a hill slope adjacent to the village of Trescléoux. It belongs to the "Terre Noires" facies and consists of grey to black marls, which contain layers of carbonate nodules parallel to the bedding. These nodules are round to oval in shape, and about three to ten centimeters in diameter [1]. Up-section, nodules become more abundant. The upper part of the section comprises the "Argovien" facies. This facies consists of an alternation of marls with marly limestones. The base of the "Argovien" is very distinct in the field, thus providing a good correlation marker. The "Argovien" facies replaces the "Terre Noires" synchronously in the whole Subalpine basin, marking the top part of the *Antecedens* ammonite-subzone. Here another 94 samples were collected within 80 meters [1].

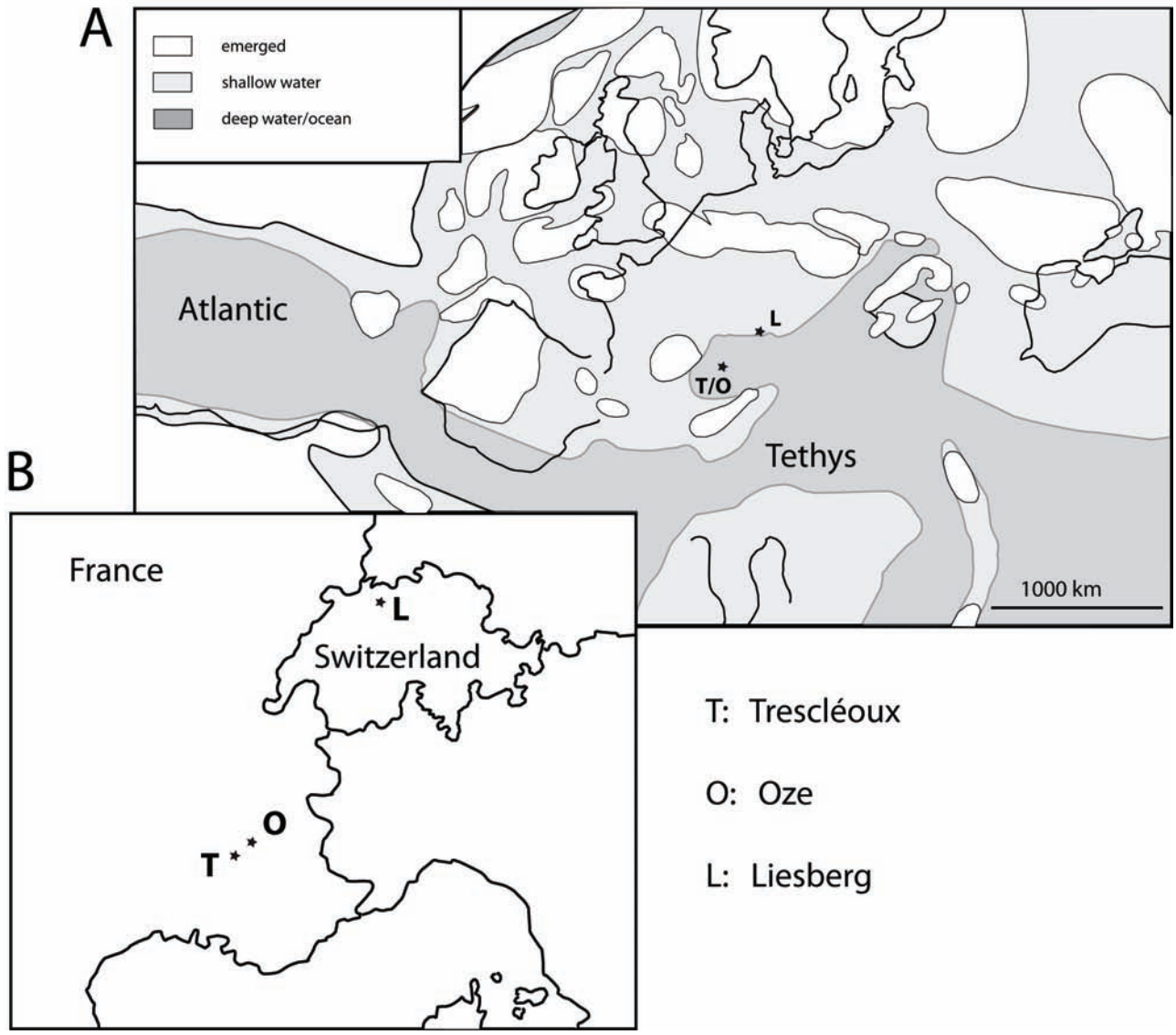

Fig. (1). Location map (**A**) and paleogeography (**B**) of the studied sections. T = Trescléoux, O = Oze. Black lines represent modern coast lines and state borders. Palaeomap modified after [77]. Location map after Louis-Schmid *et al*. [2].

Oze is situated around 50 km to the northeast of Trescléoux. Samples were taken from the top of the *Vertebrale* and the whole *Antecedens* ammonite subzone. This section is the direct stratigraphic precursor of the "Argovien" facies and could not be clearly identified and, therefore, not sampled at Trescléoux. The facies is the same as in the lower part of Trescléoux, except that the nodules are slightly bigger. 112 samples within a height of 102 meters were collected. Correlation between Trescléoux and Oze is specified by a remarkably thick bentonite layer occurring in the *Vertebrale* ammonite subzone.

The lower "Terre Noires" facies consists of dark, clayey marlstones with carbonate contents commonly between 30 and 40 wt.%. The carbonate consists of calcite dominated by micrite, but well-preserved coccoliths and parts of coccospheres are also present. Protoglobigerines can be observed as well. Macrofossils are rare but dominated by ammonites and belemnites. Carbonate nodules, with up to 80% CaCO3, are frequent in the "Terre Noires" and the Sornetan Member. They reach up to 30 centimeters in diameter. The "Terre Noires" also have slightly elevated organic carbon contents (up to 0.8 ‰ in the "Terre Noires"). In the upper part of the "Terre Noires", limestone becomes dominant [1, 2].

The "Argovien" facies is carbonate-rich, ranging between 50 and 90 wt.% $CaCO_3$, and forms an alternation of marlstones and limestones. Organic matter is a mixture of mainly marine and sparse terrestrial material based on biomarker evidence.

Detrital minerals include clays and quartz, carbonate includes micrite, coccoliths and foraminifera; macrofossils are rare and consist mainly of ammonites and belemnites. The marlstones are bedded at a decimeter- to meter-scale (according [1 - 3]).

EXPERIMENTAL

Sample Preparation

21 samples consisting of the so called "Terre Noires" from Oze (grey to black marlstone with carbonate nodules parallel to the bedding) and 8 samples from Trescléoux (grey to black marlstone with carbonate nodules parallel to the bedding in the lower part and an alteration of marlstones and limestones of the so called "Argovien" in the upper part) were treated as follows:

Fused glasses were prepared by mixing a 5:1 ratio of flux to a finely ground sample (approx. 1.5 g, after milling 30 g of a sample down to fine grains). After determination of the loss of ignition and careful homogenization the samples were transferred to Pt crucibles and melted at 1100°C in a top loading furnace (Claisse M4 Fluxer from Corporation Scientifique Claisse, Sainte-Foy, Québec, Canada) for 15 minutes. Automatic agitation ensured a good homogeneity of the melt. The melt was automatically poured into Pt plates and air cooled.

Laser Ablation Analysis

A pulsed 193 nm ArF Excimer laser (Lambda Physik, Germany) with a homogeneous beam delivery prototype system similar to a Geolas (Microlas, Germany) in combination with an ELAN 6100 DRC (Perkin Elmer, Canada) ICP-MS was used to perform the LA-ICP-MS analyses of major, minor and trace elements [35, 36]. Up to ten samples were loaded along with the glass standard NIST 610 in a 15 cm^3 ablation cell and put on the stage of a modified petrographic microscope. To the laser ablation carrier gas, helium, the make up gas argon was admixed after the ablation cell and the aerosol then carried to ICP-MS. Following methods as described by [37] and [38] data reduction was carried out using the software LAMTRACE and in-house spreadsheets. Limits of detection were calculated for each element and each analysis individually as three times the standard deviation of the background signal (measured before laser ablation) divided by element sensitivity during the respective ablation. More details of the laser ablation analyses can be found in [39].

RESULTS

All samples were measured for the following elements: Na, Mg, Al, Si, P, K, Sc, Ti, V, Cr, Mn, Fe, Co, Ni, Cu, Zn, As, Rb, Sr, Y, Zr, Nb, Mo, Ag, Cd, Sn, Sb, Cs, Ba, La, Ce, W, Tl, Pb, Bi, U. The concentration of As is rarely above the LOD (limit of detection. Sb and Tl were often not above the LOD, Mo, Ag and Cd are not considered any further, as their concentration is constantly below LOD. Table **1** lists all the concentrations and the standard deviation of the relevant elements and Fig. (**3**) illustrates examples of concentration patterns.

Studies [1, 2] report a $\partial^{13}C$ excursion in the "Argovien" facies (marls with marly limestone) from Trescléoux where samples were taken within the upper section for this study (Fig. **2**). Within the lowest sequence of Trescléoux a continuous rise of the $\partial^{13}C$-values from about 0 to 2 ‰ is evident. After an interim decrease to values around 1 ‰, $\partial^{13}C$-values oscillate around 1.5 ‰. The positive excursion in the strict sense then starts from values at around 2 ‰ and reaches values of more than 3 ‰ at its maximum. The most positive values are almost immediately followed by a negative spike down to around 0.5 ‰. Later values of around 2 to 2.5 ‰ are reached again. The most pronounced change in lithology, from the "Terre Noires" to the "Argovien", takes place as the values of $\partial^{13}C$ rise from 2 to 3%.

For the present study a representative portion of samples available from Trescléoux and Oze were used for the analysis of major, minor and trace elements. The samples were chosen in order to represent all sections of the profile according to the portions with the most pronounced changes in $\partial^{13}C$ [1].

The fluctuation or variation in concentration of the chemical elements in question are of major interest within the positive excursion in the strictest sense with a $\partial^{13}C$ rise from 2 to 3 ‰. The major elements Na, Mg and Al (Fig. **3** with Na, Mg and Al as examples) reach the highest concentrations within the excursion just before their concentrations decreases again to values as measured within the lower zones. Si and K do not show this clear rise in concentration within the $\partial^{13}C$ excursion, but again exhibit the decrease within the zone of the negative spike down to around 0.5 ‰. The fluctuation in concentrations of Si and K within the lower part of the "Terre Noires" are similar to those of Na, Mg and Al.

Table 1a. Element Concentrations in ppm with Standard Deviations in Marine Sediments as Measured by LA-ICP-MS (Three Analyses Per Average)

	TR2		TR7		TR14		TR19		TR42	
	Mean	**Std**	**Mean**	**Std**	**Mean**	**Std**	**Mean**	**Std**	**Mean**	**Std**
Na	3110	121	1550	14	2350	25.4	2900	5.8	752	14.2
Mg	9960	44.5	7800	97.2	5970	83.6	10400	131.3	4750	20.5
Al	80500	280	40800	236	36800	218	64000	144	10600	141
Si	188800	3600	93100	1110	146100	1060	156800	1150	31100	195
P	330	6.7	282	4.7	16700	215	523	5.9	189	2.5
K	17900	465	8030	113	7650	59.8	13600	336	1520	144
Sc	12.2	0.24	6.6	0.15	8.7	0.13	9.7	0.3	2.1	0.06
Ti	3650	36.7	1850	23.4	2220	17	2850	21.9	425	8
V	115	0.81	69.8	0.29	70.5	0.3	89.5	0.63	20.8	0.13
Cr	146	5.6	62.1	0.54	57.5	4.7	89.3	3.2	28.6	2.8
Mn	436	2.7	346	3.2	410	3.2	912.6	15.4	657	7.8
Fe	29200	190	17400	51.4	22700	199	44800	452	12500	119
Co	12.2	0.32	5.8	0.13	4.4	0.4	6.72	0.42	1.3	0.02
Ni	67.4	3.5	30.2	3.33	34	8.8	8.8	1.2	12.3	1.1
Cu	18.6	1	10.9	0.58	12.3	1.5	45.7	0.41	9.2	0.76
Zn	69.4	1.6	41.1	0.45	70.7	4.8	18.8	0.88	33.8	2.4
As	9.4	0.08	6.5	0.52	4.4	0.05	56.4	0.56	0.7	
Rb	98	1.9	48.6	0.81	40.6	0.55	74.4	0.85	8.8	0.05
Sr	306	3.6	370	1.1	654	5	464	2.3	424	0.98
Y	20.1	0.2	16.6	0.48	112	1.7	22.1	0.38	12.6	0.22
Zr	130	0.67	65.5	1.13	130	3	97.1	1.4	16.8	0.34
Nb	14.6	0.45	6.9	0.21	11.1	0.33	11.1	0.24	1.7	0.07
Sn	5.8	0.47	4.4	0.14	3.3	0.18	5.8	0.08	3.9	0.7
Sb			0.23	0.01						
Cs	7.8	0.14	2.9	0.05	3	0.15	505	0.14	0.38	0.01
Ba	169	2.7	83.4	0.63	77.6	1.7	140.6	2.7	41.6	0.25
La	31	0.19	21.1	0.3	121.9	1.4	29.6	0.42	11.2	0.07
Ce	59.6	0.54	36.7	0.15	279	2.8	54.8	0.42	13.1	0.03
W	1.4	0.17	0.87	0.06	0.78	0.1	1.05	0.11	0.9	0.03
Tl	0.04									
Pb	12.5	0.48	7	0.12	5.7	0.3	8	0.18	0.7	0.07
Bi	0.25	0.05	0.13	0.02	0.2	0.01	0.17	0.04	0.06	0.01
U	1.7	0.05	1.1	0.06	1.9	0.05	1.4	0.02	0.33	0.01

Average shale data from [18] and Wedepohl [75, 76].

Table 1b. Average Shale in ppm, Element/Al Ratios and Element Concentrations in ppm with Standard Deviations in Marine Sediments as Measured by LA-ICP-MS (Three Analyses Per Average)

	OZ5		OZ15		OZ25		OZ34		OZ239	
	Mean	Std	Mean	Std	Mean	Std	Mean	Std	Mean	Std
Na	2520	17.3	2350	25.4	2520	25.1	2310	19	1090	12.9
Mg	6830	76.6	5970	83.6	7730	100	5980	74.1	6280	80.9
Al	57200	407	36800	218	41200	328	49500	335	26400	426
Si	220000	4000	146100	1060	169000	1460	187400	1740	85700	1080
P	154	12.2	16700	215	230	4.4	305	4.4	169	4.3
K	11600	144	7650	59.8	8420	148	11000	56	4670	29.2
Sc	9.4	0.62	8.7	0.13	8.4	0.69	9	0.61	5.3	0.3
Ti	3150	29.4	2220	17	2210	19.3	2750	19.3	1230	20
V	93.2	2.3	70.5	0.3	69.8	1.3	87.5	10.4	54.5	0.51
Cr	87.5	5	57.5	4.7	73.8	3.3	92.7	0.77	52.9	2.8
Mn	309	4.8	410	3.2	708	13	236	5.7	310	1.6
Fe	25600	487	22700	199	66200	733	24000	76.9	13800	263
Co	8.8	0.12	4.4	0.4	5.4	0.31	7.7	0.18	1.9	0.14
Ni	51.7	4.5	34	8.8	43.9	2.7	44.5	2.1	19.5	0.7
Cu	20.3	0.88	12.3	1.5	15.9	4.9	16.8	1.2	11.8	0.57
Zn	72.3	3.7	70.7	4.8	67.4	3.1	58.4	1.4	38.9	2.4
As	3.5	0.54	4.4	0.05	3.3	0.08	5.5	0.3		
Rb	65.1	0.98	40.6	0.55	48.5	1.3	60.7	0.4	23.3	0.12
Sr	1070	12.3	654	5	331	2.6	414	1.4	461	2
Y	17.6	0.32	112	1.7	16.1	0.28	18.7	0.73	16	0.55
Zr	137	1.4	130	3	98.7	0.36	140	0.98	44	1.59
Nb	13.2	0.1	11.1	0.33	10.1	0.29	11.5	0.18	4.8	0.12
Sn	4.4	0.33	3.3	0.18	7.2	0.05	7.5	0.47	4.3	0.42
Sb							0.34	0.06		
Cs	4.8	0.11	3	0.15	3.7	0.12	4.6	0.08	0.47	0.27
Ba	128	1.71	77.6	1.7	89.7	0.68	120	0.75	51.1	0.39
La	25.5	0.13	121.9	1.4	20.6	0.32	27.2	0.11	19	0.18
Ce	47.2	0.27	279	2.8	37.3	0.22	48.1	0.65	27.9	0.2
W	1.2	0.07	0.78	0.1	0.9	0.12	0.91	0.04	0.63	0.06
Tl	0.02				0.03		0.01	0.001	0.01	
Pb	11.2	0.65	5.7	0.3	8.7	0.034	10.6	0.19	3.8	0.26
Bi	0.16	0.01	0.2	0.01	0.16	0.01	0.15	0.05	0.1	0.1
U	1.5	0.05	1.9	0.05	1.1	0.03	1.46	0.07	0.86	0.07

Table 1c. Average Shale in ppm, Element/Al Ratios and Element Concentrations in ppm with Standard Deviations in Marine Sediments as Measured by LA-ICP-MS (Three Analyses Per Average)

	OZ265		OZ272		OZ279		OZ285		OZ289	
	Mean	Std	Mean	Std	Mean	Std	Mean	Std	Mean	Std
Na	2430	14.9	2200	21.2	2400	44.3	2270	27.8	2150	42.8
Mg	7350	61.3	7300	117.5	9600	141	7490	94.3	6780	21.5
Al	58800	487	59500	908	54800	576	58290	219	60500	655
Si	195100	1660	176000	4190	159000	4465	180100	2500	179000	3180
P	288	19.8	155	6.4	352	14.8	184	6.7	216	8.9
K	13100	51.1	12500	191	12675	219	15680	253	16300	141
Sc	10.8	0.69	8.7	0.21	11.3	0.74	9.7	0.35	11	0.35
Ti	3480	9.6	3050	28.6	3290	9.8	3160	68.9	3060	11.6
V	98.2	1	93.8	2.6	96.2	1.8	97.4	1.8	104	1.3
Cr	80	5.9	115	6.6	82.4	5.5	123	2	116	6.3
Mn	214	1.2	214	2.4	252	4	253	2.2	236	3.3
Fe	27400	182	22700	292	27100	516	26500	370	25000	290
Co	6.7	0.19	6.9	0.22	8.3	0.13	9.1	0.26	8	0.32
Ni	48.8	8.2	39.5	2.98	41.7	5.4	51.3	3.7	36.9	4.3
Cu	15.9	0.71	21.7	0.23	14.9	0.9	13.1	0.86	19.2	2
Zn	55.1	1.22	90.8	1.4	51.2	1.4	65.6	0.91	95.3	3.1
As	5	0.45	4.2	0.65	2.9	0.8	4.2	0.61	3.4	0.4
Rb	73.7	1.56	78.9	0.86	72.8	1.7	84.4	0.35	95	1.7
Sr	338	0.71	395	1.46	446	1.4	417	6.1	314	1.5
Y	18.2	0.38	16.2	0.75	21.5	0.81	18.4	0.32	16.7	0.77
Zr	147	1.22	104	3.11	152	3.5	127	0.66	105	2.1
Nb	18.6	0.36	12.9	0.07	14.6	0.05	12.6	0.11	12.5	0.47
Sn	3.8	0.85	7.3	0.73	4.2	0.34	8.1	0.86	8.5	0.13
Sb	0.7	0.15	0.35							
Cs	5.9	0.26	6.0	0.11	5.6	0.19	6.2	0.04	7	0.16
Ba	127	1.2	136	1.7	142	2.7	153	2.9	163	1.69
La	26.4	0.41	26	0.45	30.4	0.3	28.8	0.26	27	0.6
Ce	46.1	0.42	43.7	0.93	51.7	1.2	49.3	0.83	46.7	0.21
W	1.3	0.18	1.2	0.16	1.2	0.15	1.2	0.09	1.4	0.19
Tl	0.14	0.06	0.01		0.07	0.01	0.01			
Pb	10.4	0.34	9	0.56	9	0.23	13.3	0.13	10.3	0.55
Bi	0.24	0.03	0.2	0.01	0.22	0.06	0.18	0.02	0.24	0.6
U	1.6	0.07	1.5	0.02	1.7	0.03	1.39	0.03	1.5	0.01

Table 1d. Average Shale in ppm, Element/Al Ratios and element Concentrations in ppm with Standard Deviations in Marine Sediments as Measured by LA-ICP-MS (Three Analyses Per Average)

	OZ294		OZ300		OZ301		OZ306		OZ310	
	Mean	**Std**	**Mean**	**Std**	**Mean**	**Std**	**Mean**	**Std**	**Mean**	**Std**
Na	1930	12.2	2200	21.6	2000	18	1660	38.4	1810	18.1
Mg	5940	55.2	5800	63	6180	85.5	6480	89.8	7040	91.7
Al	50500	578	45300	365	39200	217	51800	103	47500	307
Si	170000	2740	178100	3580	154000	2630	182000	4810	166900	1340
P	224	10.5	304	15.5	207	7.1	154	8.1	158	4.2
K	13200	206	10500	90.5	9170	92.9	13500	234	9920	153
Sc	9	0.31	8.7	0.88	7.3	0.5	9	0.3	8.5	0.3
Ti	2730	40.8	2810	24.7	2120	7.2	2620	46.1	2610	12.7
V	94	1.2	89.3	1.6	75.4	1.7	90.9	2.6	88.6	1
Cr	111	4.8	67.7	1.9	61	1.6	124	10.6	101	1.4
Mn	180	3.3	139	1.9	204	2	165	1.8	202	4
Fe	21500	386	21800	218	20100	313	21000	544	20400	178
Co	8.4	0.23	7.6	0.22	5	0.3	4.8	0.09	4.4	0.4
Ni	46.6	11.3	40.6	2.2	32.3	9.1	42.2	2.3	32.5	3.3
Cu	14.4	1.2	12.7	0.5	11.1	0.8	16.1	1	13.1	2.4
Zn	99.6	1.5	51.2	2.2	40.4	2.4	80.8	3.3	62	2.3
As	4	0.17	4.9	0.1	3.2	0.59	3.9	0.39	3.2	0.34
Rb	73.1	0.9	59.4	1.5	51.4	0.86	74.3	1.1	65.4	0.9
Sr	386	7.3	353	1.8	402	3.6	313	4.9	377	2.9
Y	19.5	0.15	17.8	0.59	16.5	0.26	16.5	0.44	17	0.31
Zr	111	2.8	122	2.8	106	1.4	97.1	0.79	115	1.8
Nb	12	0.19	13.6	0.39	11.4	0.05	11.4	0.04	10.5	0.32
Sn	8.2	0.56	3.6	0.48	3.5	0.05	7.8	0.17	7.8	0.37
Sb	0.5	0.03			0.54					
Cs	5.6	0.2	4.7	0.07	4	0.26	5.9	0.18	5.4	0.5
Ba	167	1.57	604	5.5	123	1.7	121.3	2.5	105	1.3
La	27.6	0.22	24.1	0.6	23.3	0.37	23	0.4	23.2	0.41
Ce	43.6	0.82	41.2	0.85	37.2	0.7	37.5	0.9	38.3	0.55
W	1	0.06	1.1	0.17	0.84	0.13	1.4	0.07	1.15	0.16
Tl	0.026		0.1	0.02					0.02	0.006
Pb	8.1	0.22	0.7	0.22	6.6	0.23	8.8	0.41	8.5	0.43
Bi	0.2	0.05	0.1	0.03	0.19	0.04	0.16	0.15	0.16	0.01
U	1.4	0.03	7.7	0.09	1.25	0.05	1.27	0.05	1.2	0.05

Table 1e. Average Shale in ppm, Element/Al Ratios and Element Concentrations in ppm with Standard Deviations in Marine Sediments as Measured by LA-ICP-MS (Three Analyses Per Average)

	OZ314		OZ318		OZ328		OZ330		OZ331	
	Mean	**Std**	**Mean**	**Std**	**Mean**	**Std**	**Mean**	**Std**	**Mean**	**Std**
Na	1630	19	1390	13.4	1180	324	1500	9	946	14
Mg	6540	66.3	5710	28.6	8560	152	8870	38.3	5940	30.6
Al	48500	428	38200	323	39900	318	39900	297	20500	127
Si	162200	761	116700	1220	147600	4740	117400	2230	64600	93.3
P	316	8	217	1.7	167	5.2	292	5.8	395	6.8
K	10160	68.2	8530	90.3	8820	60.2	8410	66.5	2890	21.5
Sc	8.5	0.29	6.5	0.1	7.2	0.44	7.2	0.26	3.8	0.2
Ti	2470	17	2010	34.4	1970	19	2000	36.8	976	6.5
V	84	1.1	68.4	0.79	78.8	1.2	79.9	0.55	44.6	0.34
Cr	80.1	5.1	54.6	0.56	94.3	8.1	81.8	1.5	46.4	1.5
Mn	184	0.31	197	3	210	1.4	241	2.2	412	5.1
Fe	21400	178	17800	224	20800	261	16300	249	11500	158
Co	6	0.3	2.9	0.04	4.4	0.2	4.8	0.58	4.6	0.2
Ni	38.9	3.4	24.3	1.2	30.6	1.9	30.4	3.8	15.8	2.9
Cu	17.3	3.4	11.2	0.63	15	1	14.7	0.3	9.8	2.1
Zn	71.2	2.7	31.6	2.5	55.4	2.4	48.3	2.1	34.8	2.5
As	4	0.25	2	0.24	2.6	0.9	3.3	0.29	2.9	0.6
Rb	61.7	0.51	52.1	0.99	53.6	0.17	51.1	0.08	14.2	0.15
Sr	346	2.5	332	4.38	430	2.4	499	3.7	514	2.9
Y	20.4	0.14	15.9	0.2	14.1	0.33	16.3	0.66	14	0.16
Zr	104	2.8	68.8	0.42	82	1.8	75.3	1.3	39.5	0.08
Nb	10.5	0.22	7.8	0.19	7.6	0.23	6.9	0.42	3.6	0.1
Sn	4.7	0.5	4.8	0.48	8.1	1.5	7.5	0.05	4.0	0.21
Sb	0.27	0.03					0.5			
Cs	5	0.01	3.9	0.11	4.2	0.43	3.7	0.13	0.34	0.02
Ba	102	1	75.9	0.82	80.7	0.8	81.1	0.72	41.8	0.22
La	26.1	0.3	22	0.15	19.6	0.46	21.5	0.44	15	0.2
Ce	42.4	0.89	33.3	0.43	32.7	0.06	35.8	0.66	23.2	0.35
W	1	0.11	1.3	0.1	1.4	0.98	0.82	0.11	0.52	0.12
Tl			0.02		0.08				0.01	
Pb	8	0.25	6	0.18	6.96	0.66	5.7	0.14	1.9	0.17
Bi	0.1	0.03	0.15	0.02	0.67	0.09	0.15	0.03	0.09	0.02
U	1.3	0.04	1.2	0.07	1.7	0.06	1.04	0.04	0.67	0.03

Table 1f. Average Shale in ppm, Element/Al Ratios and Element Concentrations in ppm with Standard Deviations in Marine Sediments as Measured by LA-ICP-MS (Three Analyses Per Average)

	OZ332		TRE21.5		TRE32		TRE44		TRE72	
	Mean	**Std**	**Mean**	**Std**	**Mean**	**Std**	**Mean**	**Std**	**Mean**	**Std**
Na	1170	17.8	3780	73.5	1160	501	2970	7	2550	16.9
Mg	6760	39.5	16700	61	1490	36.5	7380	30.5	7100	38.5
Al	28100	439	61400	312	1270	184.4	58700	223	61400	459
Si	83200	1680	167000	3050	5830	1680	176000	1590	163500	2050
P	1686	7	2240	13.9	174	47.6	361	1.5	167	5
K	5680	38	6260	25.6	854	462	13100	87.7	15000	63.4
Sc	6.1	0.25	11.1	0.5	0.51	0.04	9.8	0.48	10.1	0.22
Ti	1340	12.5	2700	73.7	12600	452	3120	9.2	3170	11.8
V	55.4	1.2	116.9	2.5	3	1.6	89.4	0.37	103	1.1
Cr	64.3	4.6	92.4	3.2	6.6	2.7	75	11	77.5	3.3
Mn	358	5.7	2600	20.4	210	8.2	473	6	591	6.6
Fe	16600	56.9	36700	182	520	93.7	25700	146	32700	281.7
Co	4.3	0.15	9.9	0.64	0.07	0.08	12.8	0.67	11.1	0.38
Ni	25.1	1.9	49.1	3.3	13	7.1	51.9	8.2	58.1	2.4
Cu	16.7	1.9	41.6	4.6	49.6	4.1	21.7	4.2	35.3	2.7
Zn	52.9	1.3	83	3.8	32.2	22.5	58.8	3.2	84.8	3
As	1.6		4.8	1.9	4.3		13.5	1.1	5.2	0.32
Rb	34.9	0.4	23.3	0.24	2.3	0.62	76.3	1.4	93.6	0.41
Sr	473	4	1300	5.8	419	7.7	353	1.5	318	1.2
Y	18	0.35	57.6	1.1	5.2	0.4	19.8	0.2	20.8	0.57
Zr	47.5	1.4	106	2.1	16.2	13.7	106	0.1	101	2.41
Nb	4.9	0.13	12.9	0.25	40.7	2.2	13.4	1.29	14.9	0.29
Sn	6.2	0.19	13	0.22	3.1	0.75	6.2	0.21	6.6	0.37
Sb									0.33	0.01
Cs	2.2	0.03	0.29	0.04	0.19	0.05	6	0.26	7.2	0.04
Ba	58.8	0.8	112	1.1	22.7	2.9	121	0.89	131	1.2
La	21.3	0.31	50.6	0.98	4.9	0.55	27	0.08	29.6	0.13
Ce	32	0.52	71.1	0.64	4.9	0.47	49	0.32	51	0.56
W	1.1	0.06	1.5	0.97	3.6	0.16	1.48	0.23	1.1	0.5
Tl	0.01				0.02	0.01	0.01	0.004		
Pb	4.9	0.3	4.5	0.19	11.6	0.78	9.7	0.23	11.4	0.45
Bi	0.08	0.08	0.22		0.2		0.19	0.01	0.19	0.03
U	1	0.01	2.1	0.14	0.26	0.02	1.6	0.12	1.5	0.09

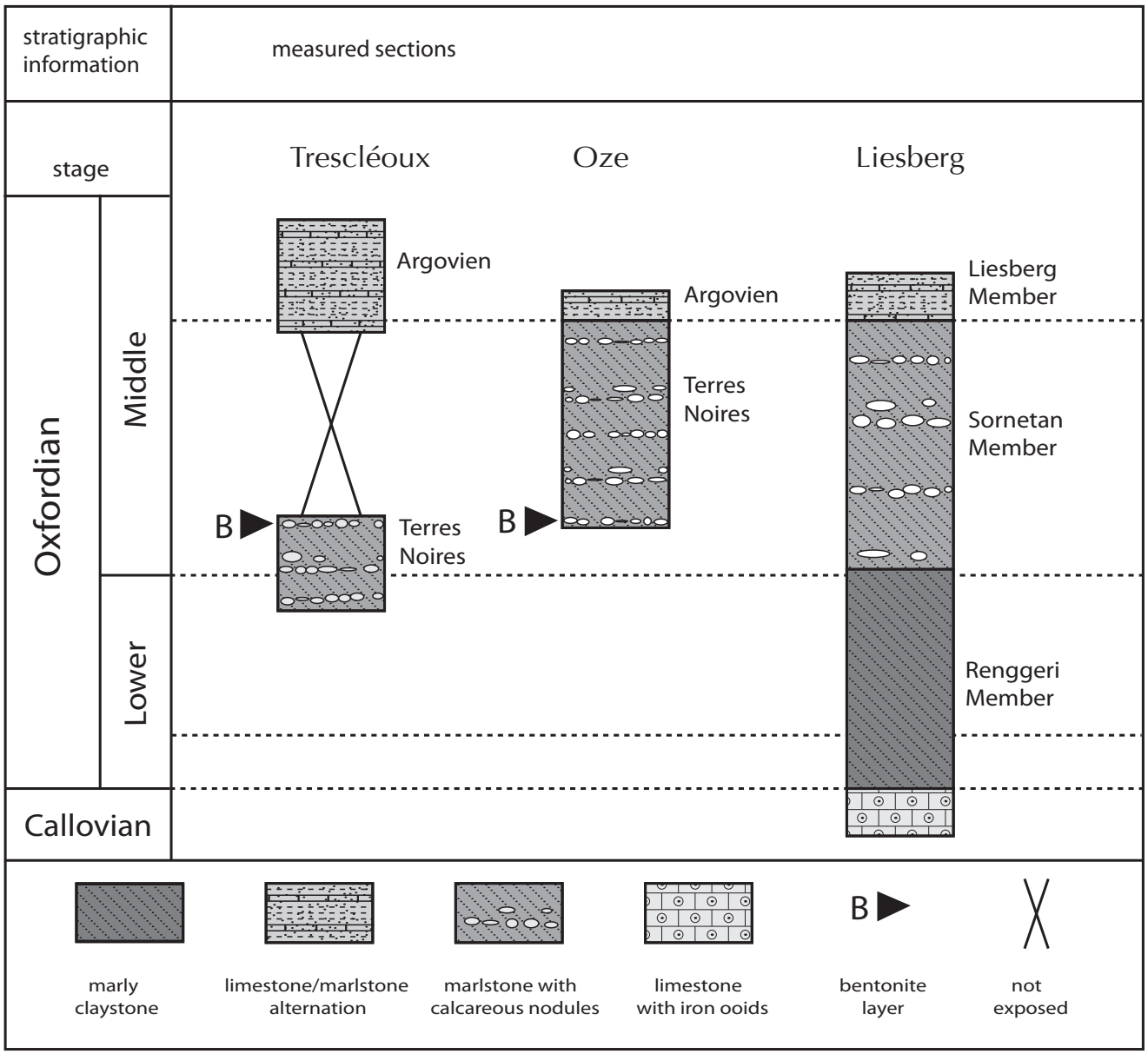

Fig. (2). Lithology and formation names of the studied sections. After Louis-Schmid *et al.* [2].

P values are as high as 2240 ppm at the upper limit of the ∂^{13}C excursion. A concentration of P as high as 16700 ppm is registered at the lower end of the "Terre Noires" (not shown in Fig. **3**). Sc, Sr, Y, La and Ce show a concentration pattern similar to P, La and Ce exhibit a distinct peak within the lower part of the profile (not shown in Fig. **3**). Rb and Cs show a concentration pattern similar to P but without the typical peak at the upper limit or the ∂^{13}C excursion.

The concentration of V and U fluctuate evenly with the distinct drop within the zone of the negative spike concerning ∂^{13}C. U solely exhibits a characteristic peak in concentration within the middle part of the profile. Cr, Co and Ni belong to this group as well but exhibit greater fluctuations within the middle part of the profile.

Ti exhibits a spike of 12600 ppm similar to P at the upper limit of the ∂^{13}C excursion. Ti fluctuates distinctly within the lower part of the profile and reaches more constant values within the part just below the ∂^{13}C excursion in the strict sense. Zr behaves similar to Ti but without the apparent spike of Ti. The variations in concentration of Nb and W resemble more or less this for Ti.

Mn and Fe have a distinct profile of their own, with high concentrations within the lower part of the section. A striking peak (Mn: 2600 ppm, Fe: 36700 ppm) occurs again similar to P at the upper limit of the ∂^{13}C excursion.

The concentrations of Cu and As are evenly distributed below the ∂^{13}C excursion. The usual spike within the ∂^{13}C excursion is as evident as for P and Ti. Bi is similar to Cu

(Na)

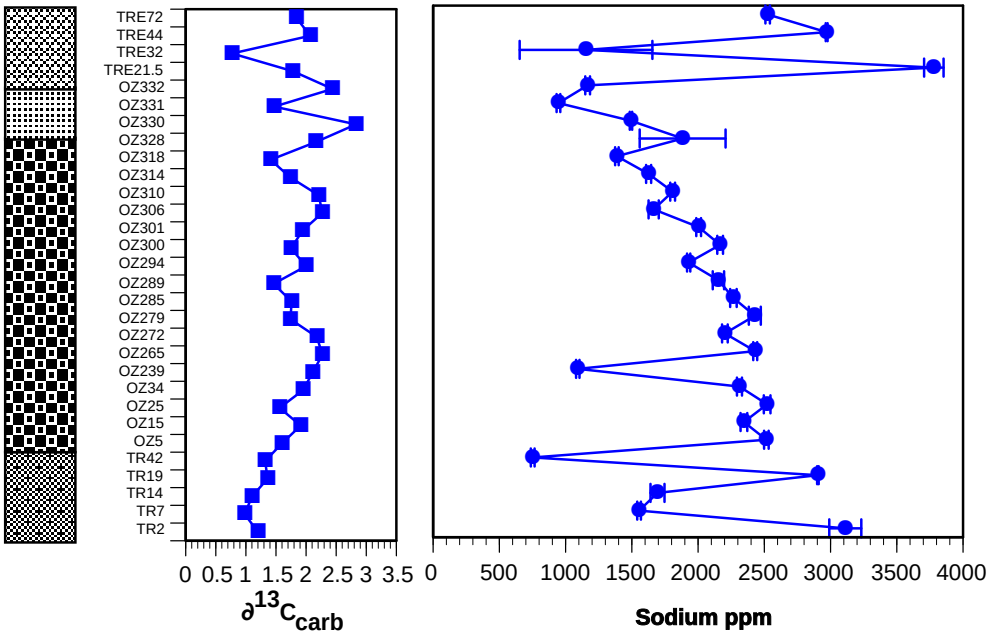

Trescléoux
Marlstone with calcareous nodules
Terres Noires

Oze
Marlstone with calcareous nodules
Terres Noires

Oze
Limestone/marlstone alternation
Argovien

Trescléoux
Limestone/marlstone alternation
Argovien

(Mg)

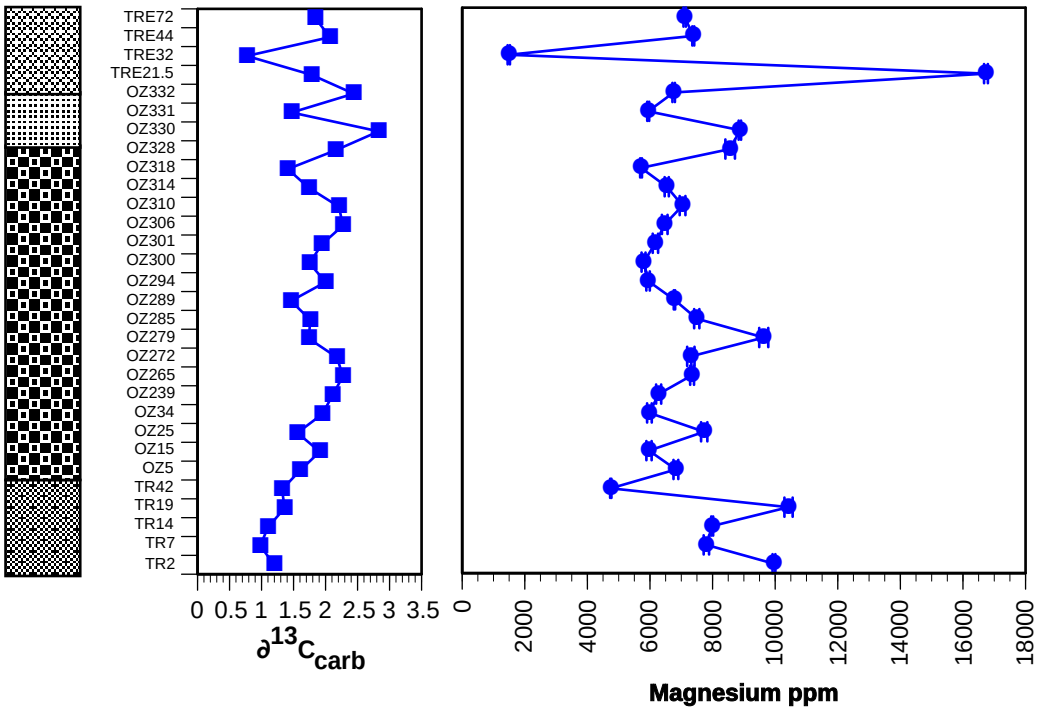

(Fig. 3) contd…..

(Ai)

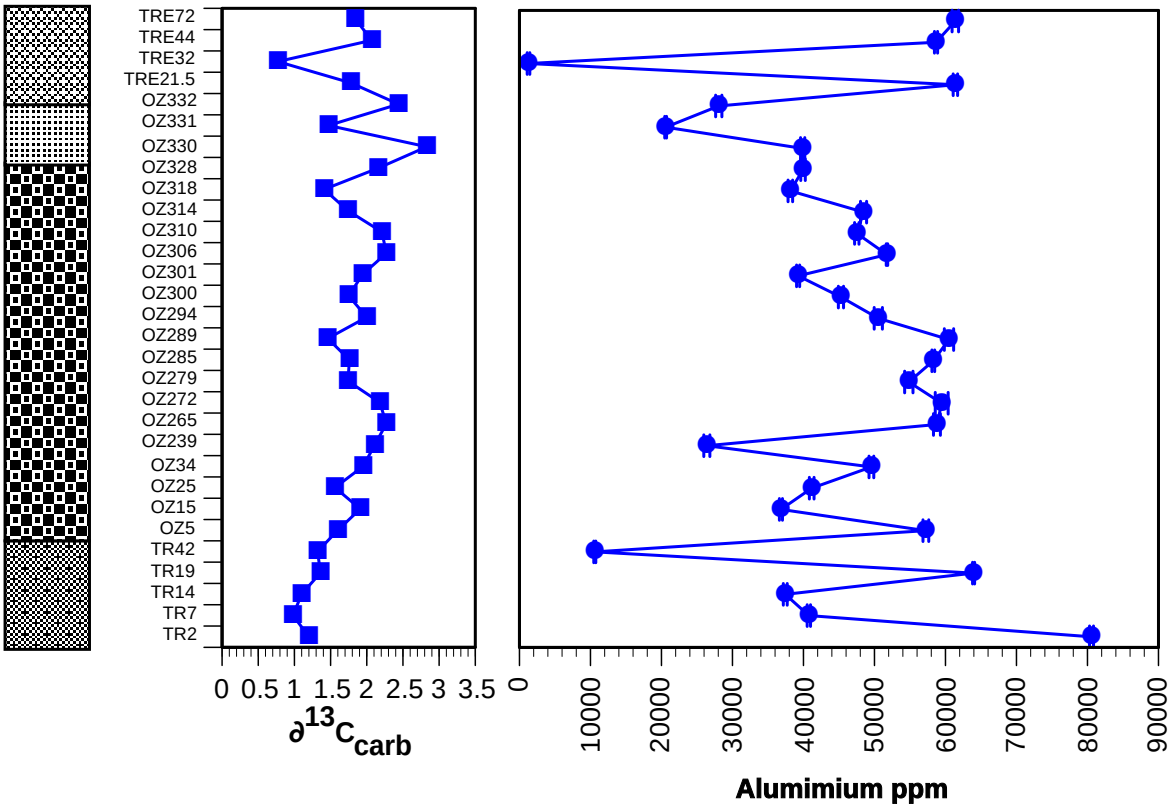

(P)

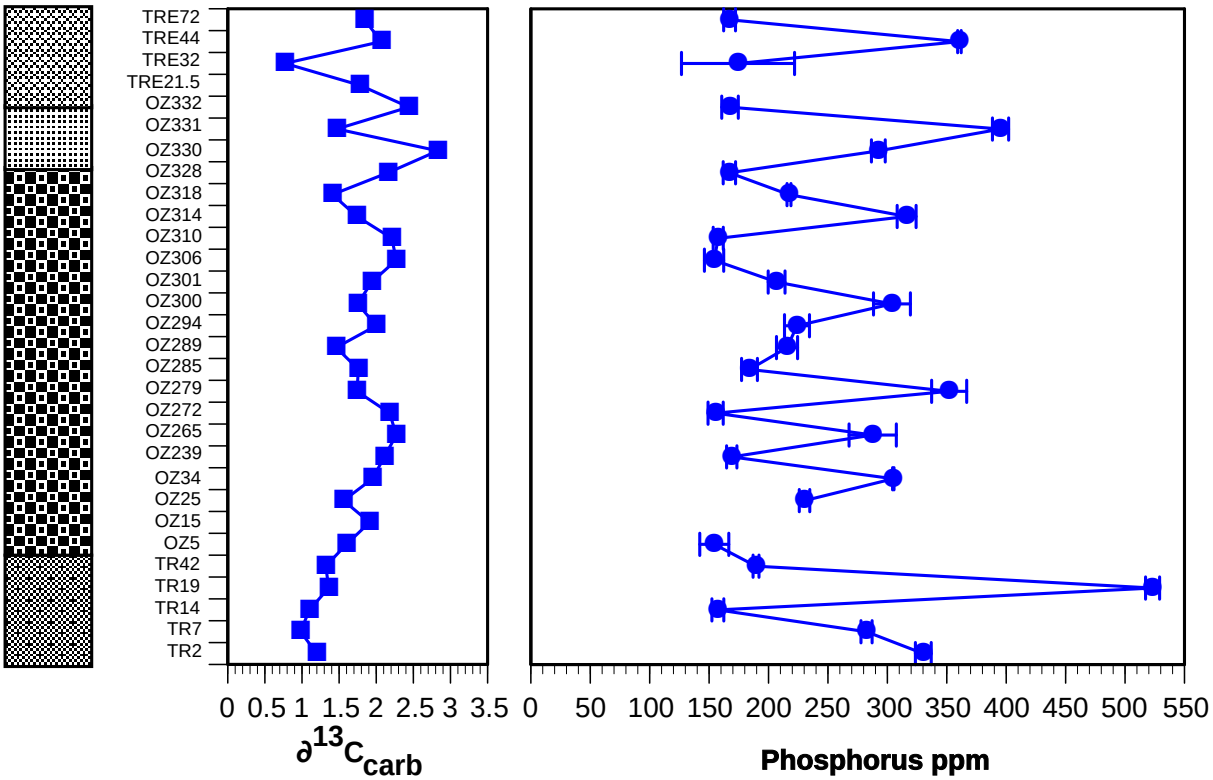

(Fig. 3) contd…..

(Ti)

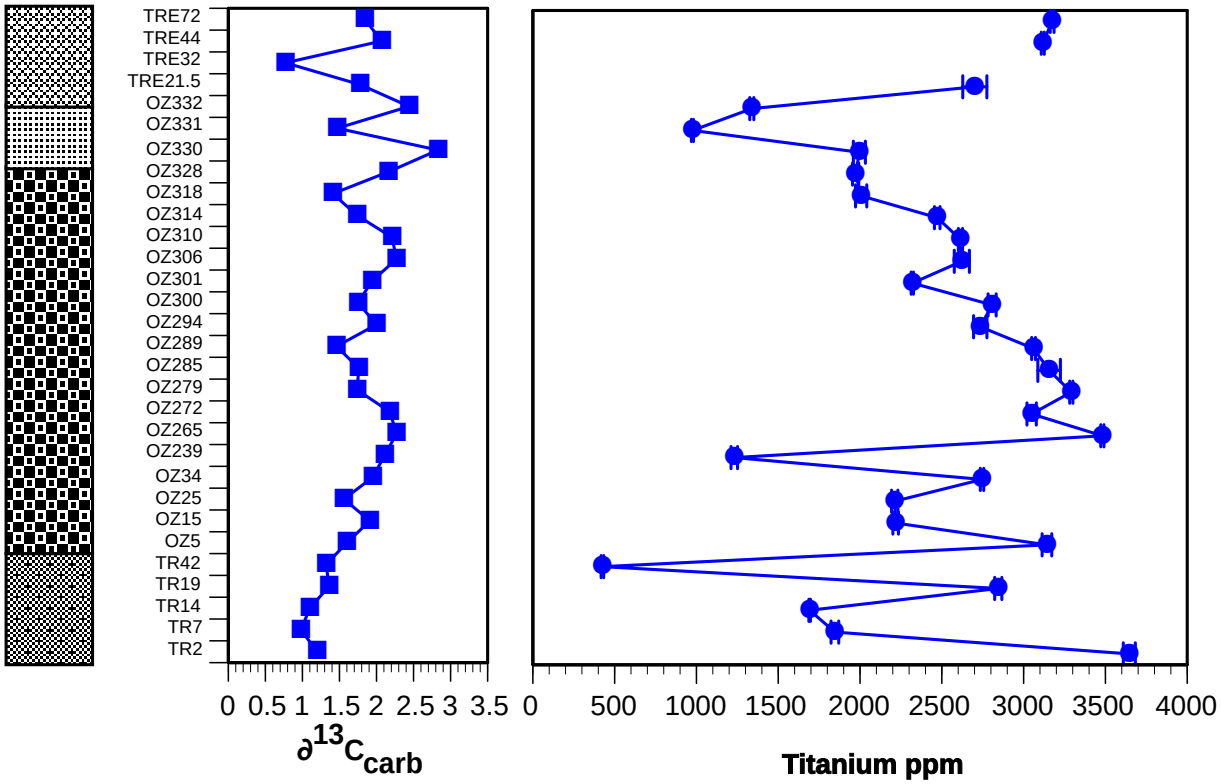

(V)

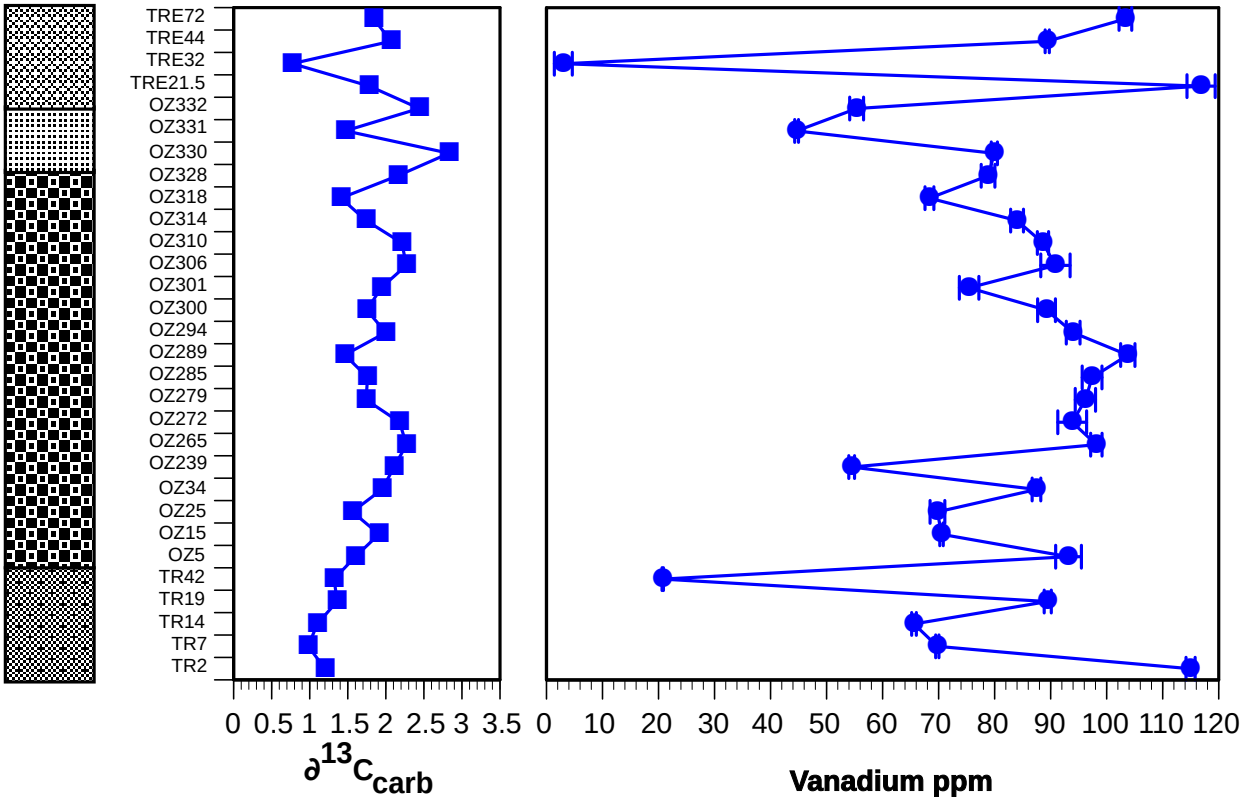

(Fig. 3) contd…..

(Mn)

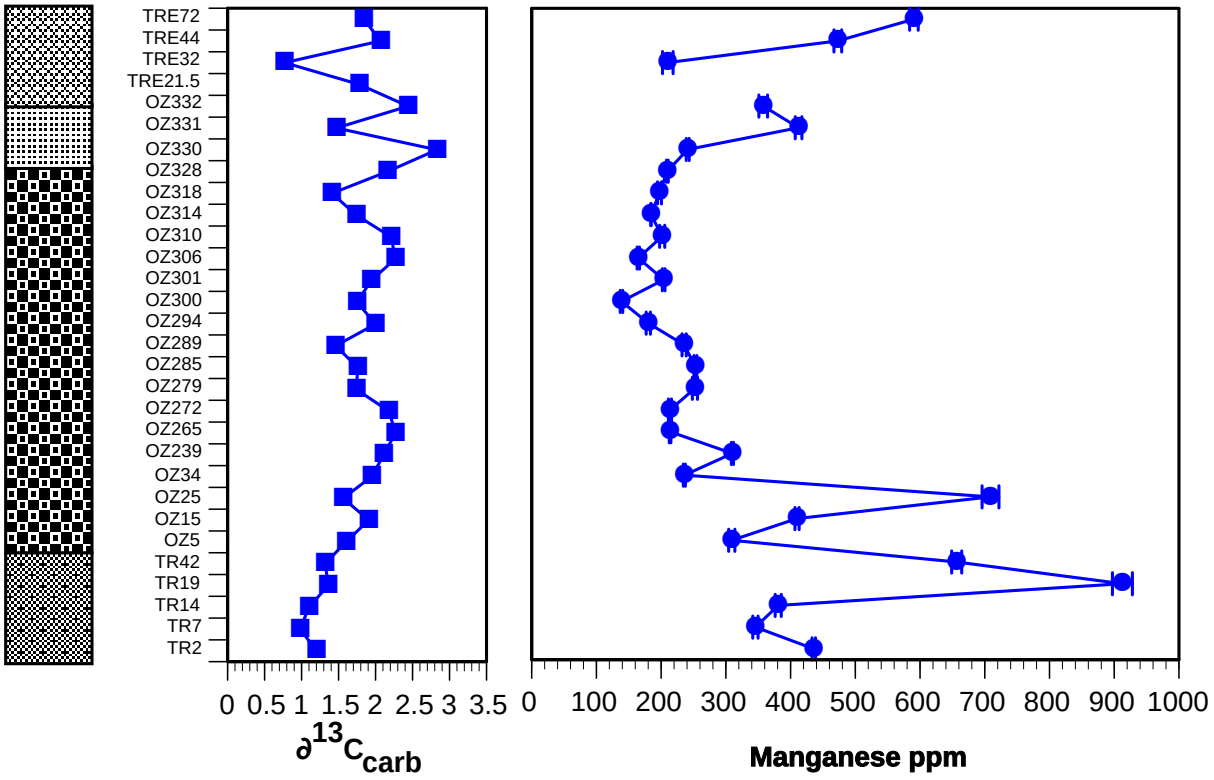

(Fe)

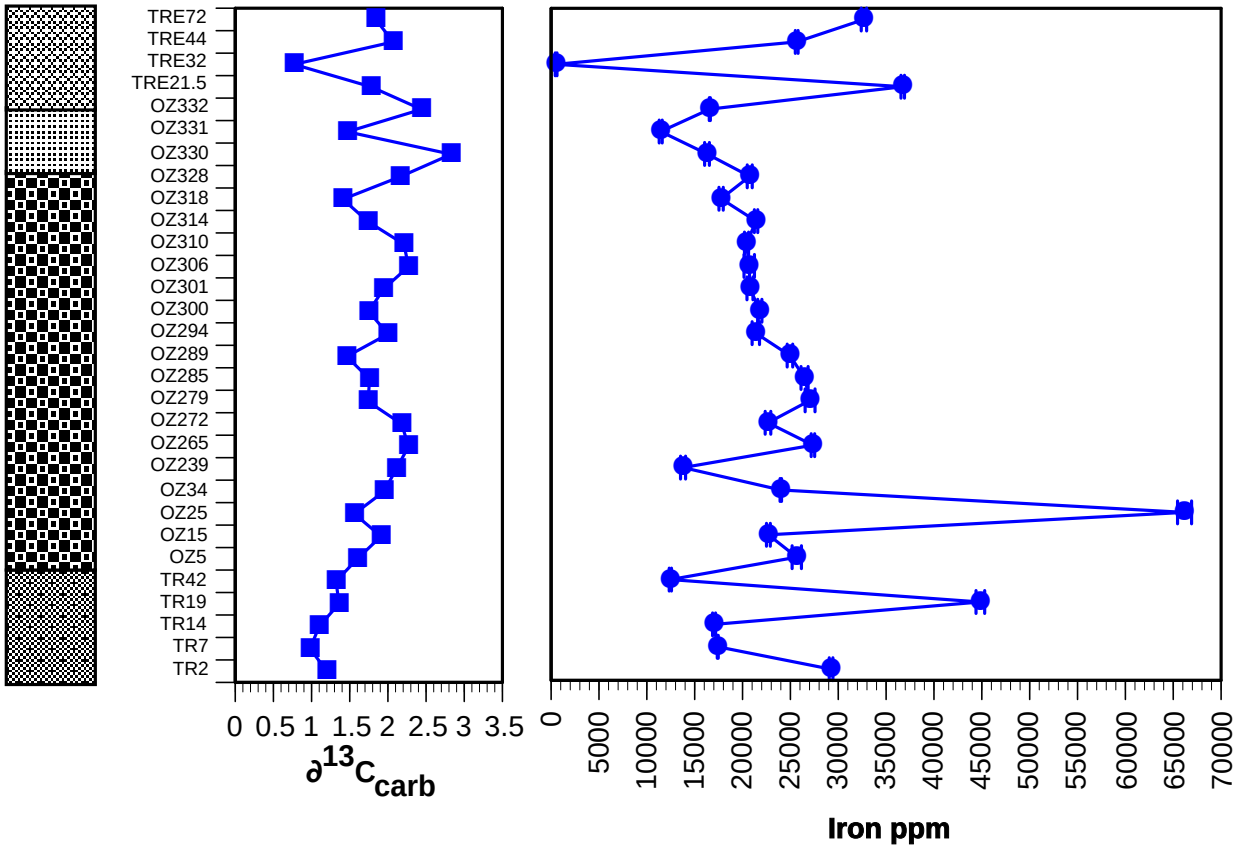

(Fig. 3) contd…..

(Cu)

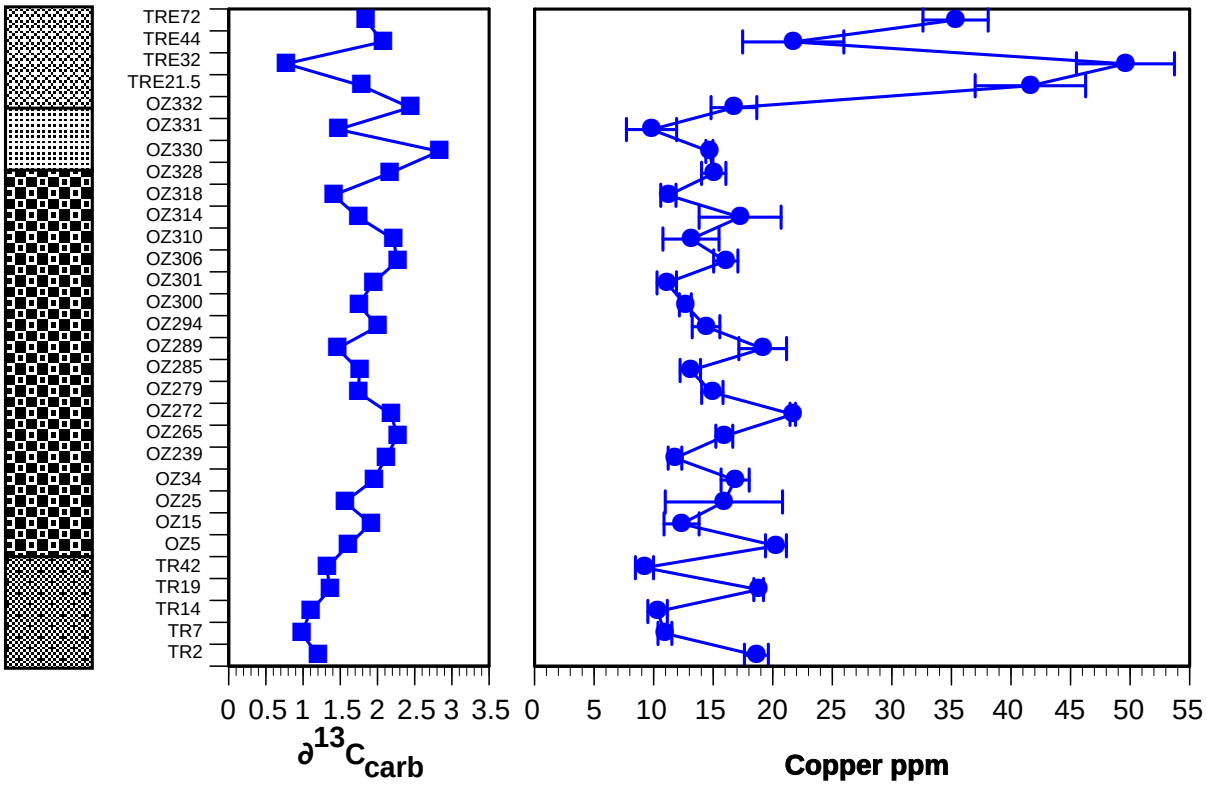

(Sr)

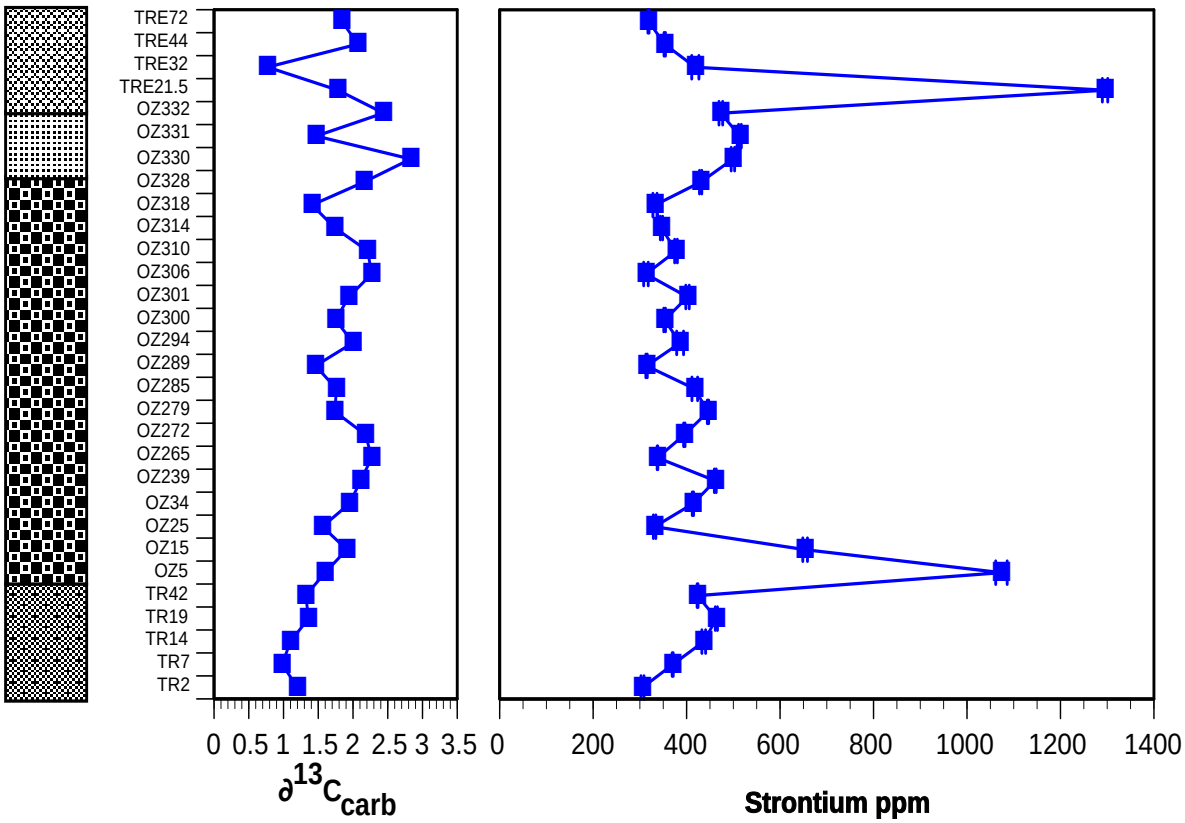

(Fig. 3) contd…..

(Ba)

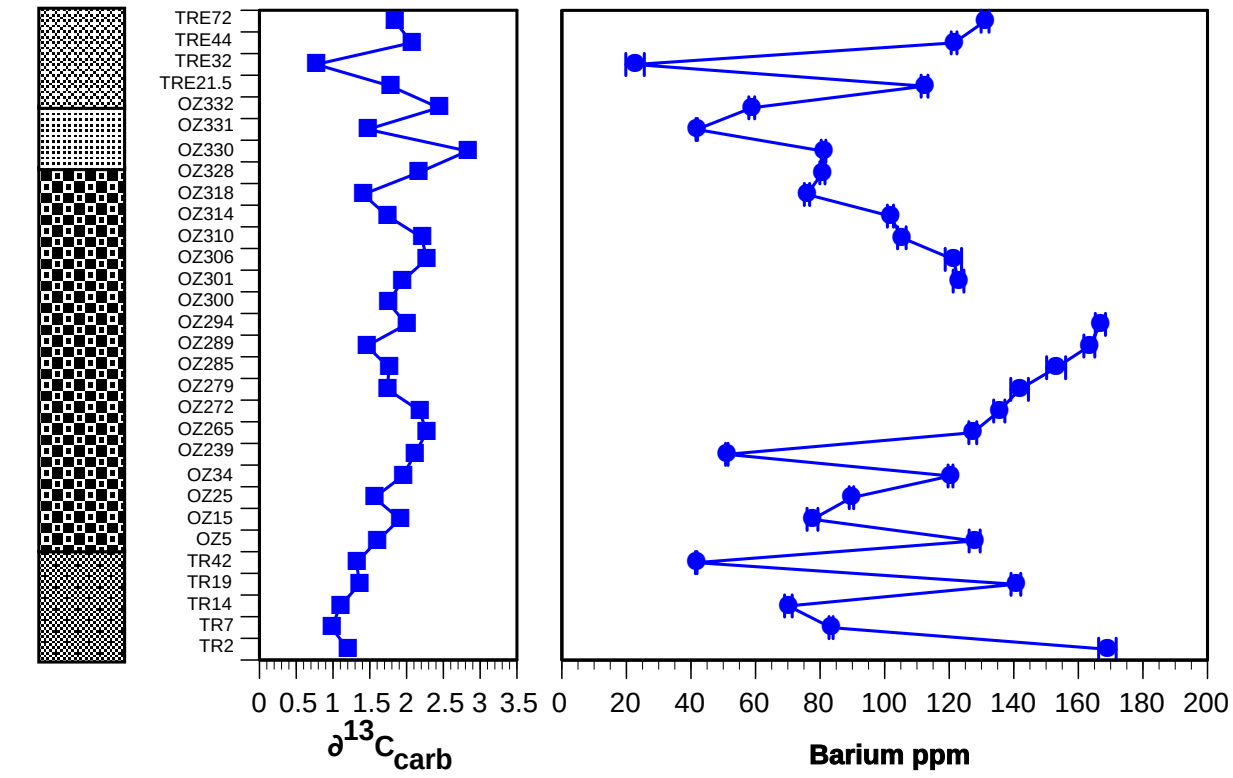

(Ce)

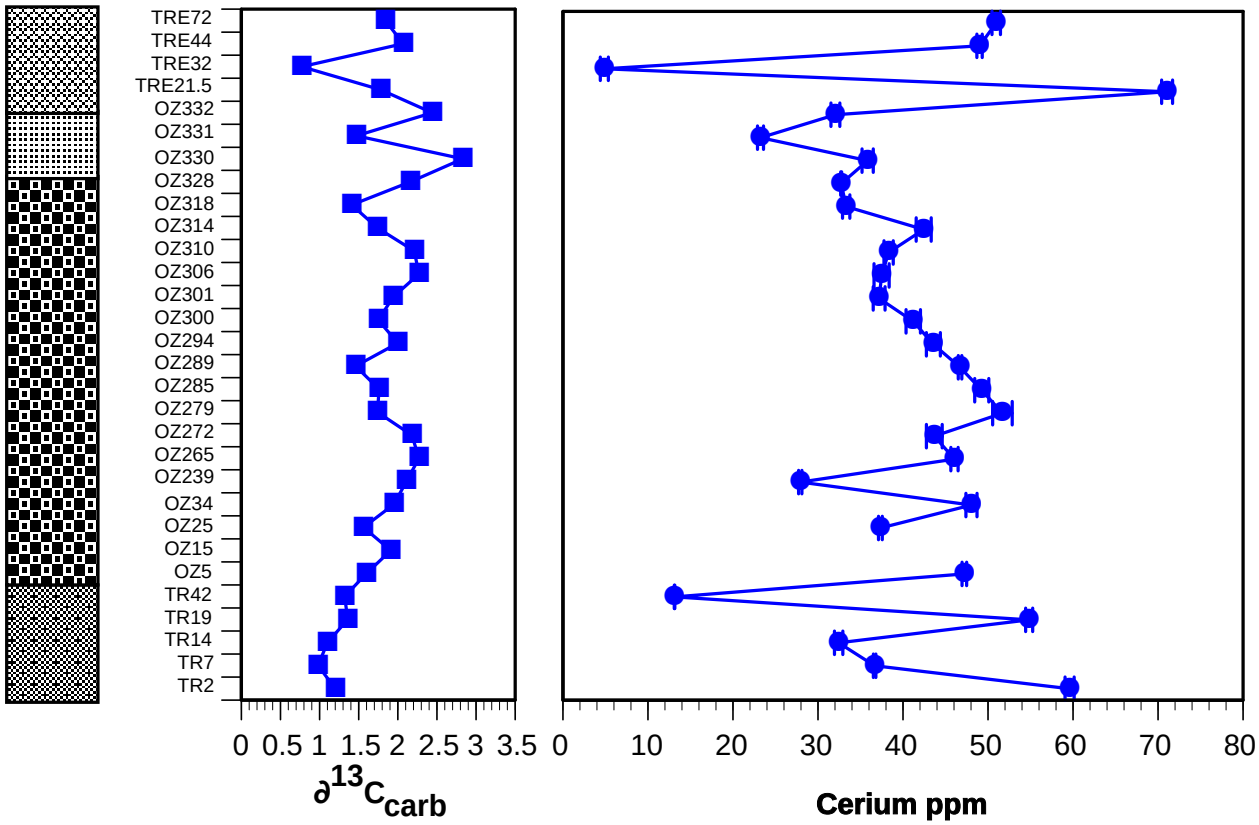

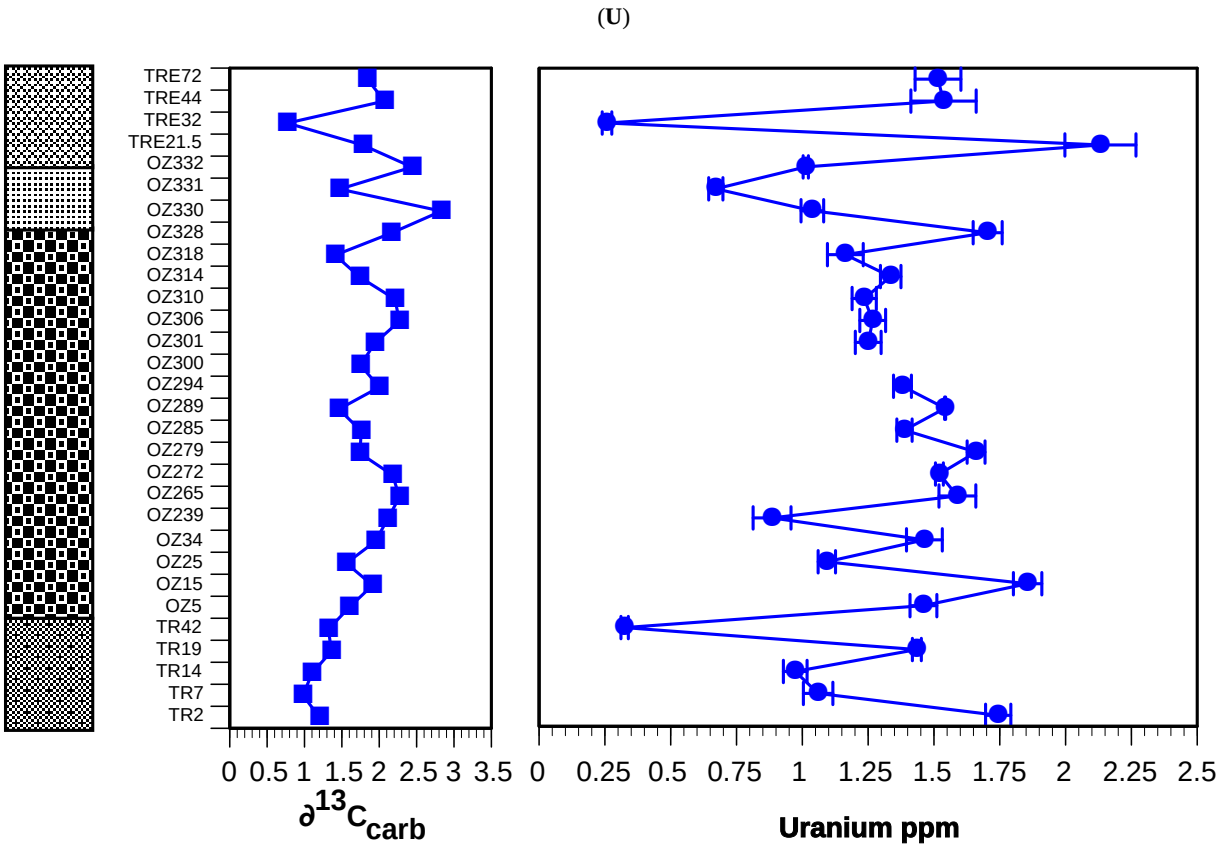

Fig. (3). Concentration patterns of the elements **Na**, **Mg**, **Al**, **P**, **Ti**, **V**, **Mn**, **Fe**, **Cu**, **Sr**, **Ba**, **Ce**, **U** with their respective error bars (proportional to their standard deviation) for all of the samples analyzed. The sample denominations are equal to their respective height within the profile.

and As and shows an obvious peak just at the beginning of the $\partial^{13}C$ excursion.

Zn does not show any distinct peak or drop in concentration within the whole profile. Sn and Pb belong to this group as well.

Sb together with Tl are elements with few statistically relevant measurements and, therefore, it is difficult to discern any particular pattern in concentrations.

Ba concentrations fluctuate within the lower part of the profile and increase steadily to values up to 600 ppm within the middle part before dropping again. No distinct peak within the $\partial^{13}C$ excursion can be seen.

Table **2** presents the major and minor element/Al ratios of average shale and marine sediments in ppm and the corresponding enrichment factors (EF) regarding Al in marine sediments. The EF is defined as follows:

$$EF = (element/Al)_{sample}/(element/Al)_{shale} \quad (1)$$

Al is the most important element essentially not affected by biological or diagenetic processes in marine environments. Al forms part of the structural component of most minerals introduced *via* fluvial and aeolian sources and, therefore, it seems to be the element of choice for quantifying the terrigenous-detrital fraction in marine environments. Another advantage of Al is its high concentration in alumosilicates and rather low abundance in seawater [18]. Any deviation from average shale composition and, therefore, either excess or depletion, is easily seen in element/Al-ratios. Any relative enrichment then is expressed by an EF>1, whereas depleted elements have an EF<1.

Among the major elements, Na and Mg show clear EF above 1 in the lower part. Another EF clearly above 1 is seen for in the uppermost part of the profile ("Argovien"). Si and K EFs oscillate constantly around 1.

Among minor and trace elements P, Sr, Y, La, Ce exhibit a peak EF in the lower part ("Terre Noires") of the profile and again in the uppermost part of the profile ("Argovien") similar to Mg. Above all Sr shows a distinct enrichment among the whole profile. V, Rb, Co, and Ni, never show a distinct enrichment with the exception within the uppermost part of the profile. Cr and Sn often exhibits enrichment factor around 2 and again a peak in EF in the "Argovien" section. As an exception Ba as well as U exhibit high EFs in the middle part of the profile and again in the uppermost part. Ti, Zr, Nb, W and including Sc oscillate the same way as Si with the exception that Ti, Zr, Nb and W are highly enriched compared to Al in the average shale in the uppermost part of the profile ("Argovien"). Fe is broadly similar to Mn with the exception of the lack of enrichment in the "Argovien". Cu, As, and Pb commonly oscillate around

Table 2a. Major and Minor Element/Al Ratios of Average Shale and Marine Sediments in ppm and Enrichment Factors in Marine Sediments

	Average Shale	Element/ Al Ratio	Element/ Al Ratio	Element/ Al Ratio	Element/ Al Ratio	Element/ Al Ratio	Element/ Al Ratio	Element/ Al Ratio
		av. shale	TR2	TR7	TR14	TR19	TR42	OZ5
Na	11870	0.13	0.039	0.038	0.045	0.045	0.071	0.044
Mg	15679	0.18	0.124	0.191	0.213	0.163	0.448	0.119
Al	88387							
Si	275322	3.11	2.34	2.28	2.44	2.45	2.93	3.79
P	698	0.008	0.004	0.007	0.004	0.008	0.018	0.003
K	29885	0.34	0.222	0.197	0.212	0.213	0.144	0.202
Sc	13	1.5*	1.518	1.61	1.65	1.52	1.95	1.64
Ti	4674	0.053	0.045	0.045	0.045	0.044	0.04	0.055
V	130	15*	14.27	17.12	17.53	13.99	19.56	16.28
Cr	90	10.2*	18.18	15.23	15.38	13.96	26.93	15.29
Mn	850	96*	54.09	84.81	101.7	142.89	619	54
Fe	48261	0.55	0.363	0.43	0.46	0.701	1.17	0.448
Co	19	2.1*	1.51	1.43	1.83	1.38	1.24	1.53
Ni	68	7.7*	8.37	7.41	9.84	7.14	11.59	9.03
Cu	45	5.1*	2.31	2.69	2.76	2.94	8.7	3.54
Zn	95	11*	8.61	10.09	11.42	8.82	31.9	12.63
As	10	1.1*	1.71	1.6	1.19	0.59	0.653	0.613
Rb	140	16*	12.17	11.92	12.11	11.63	8.26	11.37
Sr	300	34*	37.93	90.84	116.7	72.5	399.19	187.58
Y	41	4.6*	2.5	4.08	3.76	3.45	11.91	3.07
Zr	160	18*	16.17	16.07	16	15.18	15.83	23.97
Nb	18	2.0*	1.82	1.69	1.75	1.73	1.61	2.3
Sn	6.0	0.67*	0.714	1.09	1.29	0.912	3.72	0.762
Sb	1.5	0.17*		0.055				
Cs	5.5	0.62*	0.965	0.704	0.625	0.861	0.362	0.845
Ba	580	66*	20.97	20.46	18.75	22	39.25	22.34
La	40	4.5*	3.84	5.17	5.08	4.63	10.53	4.46
Ce	95	10.7*	7.4	9	8.66	8.57	12.37	8.25
W	1.8	0.20*	0.176	0.212	0.203	0.164	0.823	0.201
Tl	0.68	0.077*	0.005		0.005			0.004
Pb	22	2.5*	1.55	1.55	1.63	1.253	0.7	1.95
Bi	0.1	0.015*	0.031	0.031	0.036	0.026	0.057	0.028
U	3.7	0.42*	0.216	0.216	0.26	0.224	0.307	0.255

*Minor element/Al ratio x 10^4

Average shale data from [18] and Wedepohl [75, 76].

Table 2b. Major and Minor Element/Al Ratios of Average Shale and Marine Sediments in ppm and Enrichment Factors in Marine Sediments

	Element/Al Ratio	Element/Al Ratio	Element/Al Ratio	Element/Al Ratio	Element/Al Ratio	Element/Al Ratio	Element/Al Ratio
	OZ15	**OZ25**	**OZ34**	**OZ239**	**OZ265**	**OZ272**	**OZ279**
Na	0.064	0.061	00.47	0.041	0.041	0.037	0.044
Mg	0.162	0.188	0.121	0.238	0.125	0.123	0.176
Al							
Si	3.97	4.11	3.75	3.25	3.32	2.96	2.9
P	0.454	0.006	0.006	0.006	0.005	0.003	0.006
K	0.208	0.204	0.221	0.178	0.223	0.21	0.231
Sc	2.35	2.04	1.83	2	1.84	1.46	1.66
Ti	0.06	0.054	0.055	0.047	0.059	0.051	0.06
V	19.15	16.96	17.65	20.65	16.69	15.78	17.54
Cr	15.6	17.94	18.71	20.06	13.61	19.3	15.03
Mn	111.3	172.22	47.59	117.5	36.36	35.92	45.99
Fe	0.616	1.61	0.484	0.522	0.47	0.381	0.049
Co	1.2	1.31	1.54	0.728	1.14	1.166	1.51
Ni	9.23	10.66	8.99	7.38	8.3	6.65	7.61
Cu	3.35	3.86	3.4	4.47	2.71	3.65	2.72
Zn	19.21	16.38	11.79	14.75	9.36	15.27	9.34
As	1.19	0.81	1.12	0.45	0.85	0.701	0.53
Rb	11.03	11.78	12.34	8.82	12.54	13.27	13.27
Sr	177.5	80.55	83.43	174.8	57.44	81.3	81.3
Y	30.35	3.9	3.77	6.06	3.1	2.72	3.92
Zr	35.42	23.98	28.32	16.69	24.93	17.47	27.72
Nb	3.1	2.47	2.31	1.81	3.16	2.18	2.666
Sn	0.9	1.74	1.51	1.64	0.64	1.23	0.773
Sb			0.068		0.123	0.058	
Cs	0.82	0.9	0.93	0.18	1.01	1.01	1.03
Ba	21.08	21.78	24.29	19.36	21.65	22.78	25.86
La	33.1	2.01	5.49	7.22	4.49	4.37	5.55
Ce	75.77	9.07	9.69	10.58	7.83	7.35	9.43
W	0.21	0.218	0.18	0.24	0.127	0.192	0.221
Tl		0.007	0.002	0.005	0.024	0.001	0.012
Pb	1.54	2.12	2.13	1.43	1.773	1.514	1.65
Bi	0.055	0.04	0.034	0.04	0.04	0.032	0.0141
U	0.504	0.266	0.295	0.335	0.27	0.256	0.303

Table 2c. Major and Minor Element/Al Ratios of Average Shale and Marine Sediments in ppm and Enrichment Factors in Marine Sediments

	Element/ Al Ratio	Element/ Al Ratio	Element/ Al Ratio	Element/ Al Ratio	Element/ Al Ratio	Element/ Al Ratio	Element/ Al Ratio
	OZ285	**OZ289**	**OZ94**	**OZ300**	**OZ301**	**OZ306**	**OZ310**
Na	0.039	0.036	0.038	0.048	0.051	0.032	0.038
Mg	0.123	0.112	0118	0.118	0.157	0.125	0.148
Al							
Si	3.39	2.96	3.37	3.93	3.93	3.52	3.51
P	0.003	0.004	0.004	0.007	0.005	0.003	0.003
K	0.269	0.27	0.26	0231	0.234	0.26	0.209
Sc	1.66	1.78	1.78	1.92	1.86	1.74	1.79
Ti	0.54	0.054	0.054	0.062	0.059	0.051	0.055
V	16.71	17.15	18.6	19.74	19.22	17.55	18.65
Cr	21.09	19.18	21.92	14.94	15.52	24	21.3
Mn	43.39	39.94	35.65	30.63	51.96	31.83	42.44
Fe	0.454	0.412	0.42	0.48	0.529	0.4	0.43
Co	1.56	1.32	1.65	1.67	1.26	0.916	0.93
Ni	8.8	6.1	9.22	8.97	8.23	8.15	6.83
Cu	2.24	3.17	2.85	2.8	2.83	3.1	2.76
Zn	11.26	15.75	19.71	11.32	10.29	15.6	13.05
As	0.723	0.56	0.79	1.09	0.811	0.75	0.666
Rb	14.48	15.7	14.47	13.11	13.1	14.35	13.78
Sr	71.63	51.96	76.41	77.96	102.7	60.78	79.43
Y	3.15	2.76	3.86	3.94	4.21	3.18	3.59
Zr	21.74	17.41	21.95	27.04	27.04	18.76	24.13
Nb	2.16	2.07	2.36	3.01	2.91	2.2	2.2
Sn	1.39	1.41	1.61	0.79	0.89	1.51	1.47
Sb			0.09		0.137		
Cs	1.06	1.15	1.11	1.05	1.02	1.14	1.14
Ba	26.27	27	33	133.3	31.31	23.43	22.17
La	4.94	4.47	5.47	5.32	5.93	4.44	4.89
Ce	8.45	7.72	8.62	9.1	9.78	7.24	8.07
W	0.212	0.223	0.204	0.244	0.215	0.261	0.26
Tl	0.002		0.005	0.023			
Pb	2.28	1.71	1.59	0.154	1.69	1.7	1.66
Bi	0.031	0.04	0.04	0.023	0.048	0.031	0.034
U	0.238	0.255	0.273	1.7	0.319	0.245	0.26

Table 2d. Major and Minor Element/Al Ratios of Average Shale and Marine Sediments in ppm and Enrichment Factors in Marine Sediments

	Element/ Al Ratio	Element/ Al Ratio	Element/ Al Ratio	Element/ Al Ratio	Element/ Al Ratio	Element/ Al Ratio	Element/ Al Ratio
	OZ314	**OZ318**	**O328**	**OZ330**	**OZ331**	**OZ332**	**TRE21.5**
Na	0.034	0.036	0.047	0.037	0.046	0.042	0.062
Mg	0.135	0.15	0.214	0.222	0.289	0.241	0.273
Al							
Si	3.35	3.06	3.7	2.94	3.14	2.96	2.73
P	0.007	0.006	0.004	0.007	0.019	0.006	0.037
K	0.21	0.224	0.221	0.211	0.14	0.202	0.102
Sc	1.76	1.7	1.8	1.8	1.84	2.16	1.803
Ti	0.051	0.053	0.049	0.05	0.047	0.048	0.044
V	17.33	17.92	19.74	20.04	21.69	19.72	19.03
Cr	16.53	14.31	23.6	20.52	22.53	22.92	15.06
Mn	38.03	51.75	52.48	60.43	200.3	127.4	422.8
Fe	0.44	0.467	0.52	0.41	0.556	0.591	0.6
Co	1.24	0.756	1.1	1.2	2.23	1.546	1.62
Ni	8.02	6.388	7.67	7.63	7.66	8.94	8.01
Cu	3.56	2.95	3.77	3.68	4.77	5.96	6.78
Zn	14.7	8.29	13.88	12.12	16.91	18.85	13.52
As	0.826	0.537	0.64	0.815	1.43	0.585	0.777
Rb	12.72	13.65	13.41	12.81	6.9	12.42	3.8
Sr	71.46	87.1	107.7	125.1	249.7	168.6	211
Y	4.2	4.16	3.54	4.09	6.78	6.42	9.39
Zr	21.36	18.04	20.52	18.87	19.17	16.93	17.29
Nb	2.17	2.05	1.89	1.73	1.75	1.76	2.09
Sn	0.98	1.25	2.02	1.89	1.95	2.22	2.12
Sb	0.056			0.127			
Cs	1.04	1.03	1.04	0.932	0.166	0.79	0.047
Ba	21	19.9	20.21	20.32	20.29	20.96	18.3
La	5.39	5.77	4.9	5.39	7.274	7.6	8.24
Ce	8.76	8.73	8.2	8.99	11.29	11.42	11.58
W	0.202	0.328	0.34	0.207	0.255	0.39	0.244
Tl		0.004	0.02		0.007	0.004	
Pb	1.66	1.58	1.74	1.42	0.944	1.74	0.73
Bi	0.025	0.039	0.167	0.038	0.043	0.03	0.035
U	0.28	0.305	0.427	0.26	0.326	0.361	0.347

Table 2e. Major and Minor Element/Al Ratios of Average Shale and Marine Sediments in ppm and Enrichment Factors in Marine Sediments

	Element/ Al Ratio	Element/ Al Ratio	Element/ Al Ratio
	TRE32	**TRE44**	**TRE72**
Na	0.906	0.051	0.041
Mg	1.17	0.126	0.116
Al			
Si	4.58	3	2.66
P	0.137	0.006	0.0003
K	0.67	0.222	0.244
Sc	4	1.68	1.64
Ti	9.9	0.053	0.052
V	23.6	15.24	16.84
Cr	57.79	12.78	12.63
Mn	1650.9	80.62	96.2
Fe	0.408	0.44	0.53
Co	5.36	2.18	1.81
Ni	101.9	8.85	9.47
Cu	389.5	3.7	5.76
Zn	253.15	10.02	13.81
As	33.94	2.31	0.844
Rb	18.1	13.01	15.24
Sr	3287	60.21	51.87
Y	41.12	3.38	3.39
Zr	126.8	18.13	16.44
Nb	319.8	2.29	2.43
Sn	24.73	1.06	1.07
Sb			0.054
Cs	1.47	1.02	1.17
Ba	178	20.71	21.36
La	38.74	4.49	4.83
Ce	38.22	8.35	8.3
W	28.04	0.252	0.184
Tl		0.001	
Pb	91.34	1.65	1.853
Bi	1.63	0.032	0.031
U	2.03	0.262	0.247

Table 2f. Major and Minor Element/Al Ratios of Average Shale and Marine Sediments in ppm and Enrichment Factors in Marine Sediments

	EF TR2	EF TR7	EF TR14	EF TR19	EF TR42	EF OZ5	EF OZ15	EF OZ25
Na	0.288	0.284	0.337	0.338	0.528	0.327	0.474	0.456
Mg	0.637	1.08	1.2	0.919	2.52	0.672	0.914	1.06
Al								
Si	0.752	0.733	0.782	0.787	0.94	1.22	1.27	1.32
P	0.519	0.878	0.532	1.04	2.26	0.341	57.49	0.708
K	0.656	0583	0.628	0.629	0.425	0.599	0.615	0.605
Sc	1.03	1.1	1.12	1.04	1.33	1.12	1.6	1.38
Ti	0.856	0.857	0.855	0.841	0.758	1.04	1.14	1.02
V	0.97	1.16	1.19	0.951	1.33	1.11	1.3	1.15
Cr	1.79	1.5	1.51	1.37	2.65	1.5	1.53	1.76
Mn	0.562	0.882	1.06	1.48	6.44	0.56	1.16	1.79
Fe	0.665	0.782	0.833	1.28	2.15	0.821	1.13	2.95
Co	0.703	0.833	0.851	0.64	0.577	0.711	0.558	0.61
Ni	1.087	0.963	1.28	0.928	1.51	1.17	1.2	1.39
Cu	0.454	0.528	0.524	0.578	1.71	0.696	0.658	0.759
Zn	0.801	0.938	1.06	0.821	2.97	1.18	1.79	1.52
As	1.034	1.41	1.06	0.582	0.577	0.542	1.05	0.714
Rb	0.768	0.752	0.765	0.734	0.522	0.718	0.696	0.743
Sr	1.12	2.68	3.44	2.14	11.76	5.53	5.23	2.37
Y	0.538	0.878	0.81	0.744	2.57	0.662	6.54	0.846
Zr	0.893	0.888	0.884	0.839	0.874	1.32	1.96	1.325
Nb	0.892	0.831	0.861	0.851	0.79	1.13	1.52	1.12
Sn	1.05	1.61	1.91	1.34	5.48	1.12	1.32	2.566
Sb		0.326						
Cs	1.5	1.13	1	1.38	0.582	1.36	1.31	1.44
Ba	0.332	0.312	0.286	0.335	0.598	0.34	0.321	0.332
La	0.849	1.14	1.12	1.02	2.33	0.99	7.31	1.11
Ce	0.688	0.837	0.806	0.798	1.15	0.77	7.05	0.844
W	0.866	1.01	0.999	0.807	4.04	0.99	1.03	1.07
Tl	0.06		0.028			0.048		0.095
Pb	0.624	0.69	0.656	0.503	0.281	0.783	0.617	0.851
Bi	2.78	2.81	3.21	2.28	5.04	2.44	4.9	3.53
U	0.517	0.62	0.621	0.536	0.733	0.609	1.2	0.634

EF: Enrichment factor.

Table 2g. Major and Minor Element/Al Ratios of Average Shale and Marine Sediments in ppm and Enrichment Factors in Marine Sediments

	EF OZ34	EF OZ239	EF OZ265	EF OZ272	EF OZ279	EF OZ285	EF OZ289	EF OZ294
Na	0.347	0.308	0.308	0.276	0.33	0.29	0.265	0.284
Mg	0.68	1.34	0.704	0.693	0.99	0.725	0.632	0.662
Al								
Si	1.21	1.04	1.065	0.95	0.93	0.993	0.952	1.08
P	0.779	0.811	0.619	0.331	0.813	0.4	0.451	0.561
K	0.654	0.523	0.66	0.621	0.684	0.796	0.798	0.77
Sc	1.24	1.36	1.25	0.99	1.4	1.13	1.24	1.21
Ti	1.05	0.882	1.12	0.97	1.14	1.02	0.958	1.02
V	1.2	1.4	1.14	1.07	1.19	1.14	1.17	1.27
Cr	1.84	1.97	1.34	1.9	1.48	2.07	1.88	2.15
Mn	0.5	1.22	0.378	0.374	0.478	0.451	0.405	0.371
Fe	0.887	0.957	0.852	0.699	0.904	0.832	0.755	0.775
Co	0.718	0.338	0.531	0.542	0.701	0.726	0.612	0.769
Ni	1.17	0.959	1.08	0.864	0.989	1.14	0.792	1.198
Cu	0.667	0.877	0.532	0.716	0.535	0.441	0.622	0.56
Zn	1.1	1.37	0.871	1.42	0.869	1.05	1.47	1.83
As	0.986	0.398	0.753	0.619	0.464	0.639	0.495	0.7
Rb	0.773	0.557	0.792	0.838	0.838	0.914	0.991	0.914
Sr	2.46	5.15	1.69	1.96	2.4	2.11	1.53	2.25
Y	0.813	1.31	0.667	0.586	0.845	0.679	0.595	0.832
Zr	1.56	0.922	1.38	0.965	1.53	1.2	0.962	1.21
Nb	1.14	0.889	1.55	1.07	1.31	1.06	1.02	1.16
Sn	2.22	2.41	0.944	1.81	1.14	2.04	2.07	2.38
Sb	0.403		0.728	0.342				0.533
Cs	1.49	0.287	1.62	1.62	1.65	1.7	1.85	1.79
Ba	0.37	0.295	0.33	0.347	0.394	0.4	0.412	0.503
La	1.21	1.6	0.992	0.967	1.23	1.09	0.987	1.208
Ce	0.902	0.984	0.729	0.683	0.877	0.786	0.718	0.802
W	0.901	1.18	1.07	0.942	1.085	1.04	1.1	1
Tl	0.03	0.059	0.318	0.011	0.158	0.031		0.067
Pb	0.857	0.573	0.712	0.608	0.662	0.917	0.685	0.64
Bi	3.01	3.49	3.525	2.82	3.59	2.76	3.502	3.54
U	0.705	0.801	0.645	0.611	0.723	0.569	0.609	0.65

Table 2h. Major and Minor Element/Al Ratios of Average Shale and Marine Sediments in ppm and Enrichment Factors in Marine Sediments

	EF OZ300	EF OZ301	EF OZ306	EF OZ310	EF OZ314	EF OZ318	EF OZ328	EF OZ330
Na	0.356	0.38	0.239	0.283	0.25	0.271	0.351	0.279
Mg	0.721	0.887	0.705	0.835	0.76	0.844	1.21	1.25
Al								
Si	1.263	1.26	1.13	1.13	1.08	0.982	1.19	0.945
P	0.85	0.667	0.377	0.42	0.826	0.721	0.53	0.928
K	0.683	0.691	0.772	0.618	0.62	0.661	0.653	0.623
Sc	1.30	1.27	1.18	1.22	1.2	1.15	1.23	1.22
Ti	1.17	1.12	0.958	1.04	0.964	0.995	0.934	0.946
V	1.34	1.31	1.19	1.27	1.18	1.22	1.34	1.36
Cr	1.47	1.52	2.36	2.09	1.62	1.41	2.32	2.02
Mn	0.319	0.54	0.331	0.441	0.395	0.538	0.546	0.628
Fe	0.882	0.969	0.732	0.787	0.809	0.853	0.952	0.748
Co	0.778	0.587	0.426	0.431	0.577	0.352	0.513	0.558
Ni	1.17	1.07	1.06	0.888	1.04	0.83	0.997	0.992
Cu	0.549	0.555	0.609	0.543	0.699	0.578	0.74	0.723
Zn	1.05	0.958	1.45	1.21	1.367	0.772	1.29	1.13
As	0.962	0.717	0.66	0.588	0.73	0.474	0.565	0.72
Rb	0.828	0.827	0.906	0.87	0.803	0.862	0.847	0.809
Sr	2.297	3.02	1.78	2.34	2.11	2.57	3.17	3.69
Y	0.848	0.907	0.686	0.773	0.906	0.897	0.763	0.881
Zr	1.49	1.49	1.04	1.33	1.18	0.997	1.13	1.04
Nb	1.48	1.43	1.08	1.08	1.06	1.01	0.93	0.85
Sn	1.17	1.32	2.22	2.17	1.44	1.84	2.97	2.75
Sb		0.808			0.33			0.75
Cs	1.69	1.64	1.83	1.83	1.67	1.649	1.67	1.5
Ba	2.03	0.477	0.36	0.39	0.32	0.303	0.308	0.31
La	1.18	1.31	0.98	1.08	1.19	1.28	1.083	1.19
Ce	0.847	0.882	0.674	0.75	0.815	0.812	0.762	0.836
W	1.2	1.06	1.28	1.19	1.16	1.609	1.67	1.02
Tl	0.293				0.042	0.055	0.257	0.088
Pb	0.062	0.677	0.681	0.666	0.721	0.637	0.7	0.379
Bi	1.99	4.24	2.77	2.21	2.21	3.48	14.75	3.34
U	4.06	0.761	0.585	0.621	0.658	0.728	1.02	0.622

Table 2i. Major and Minor Element/Al Ratios of Average Shale and Marine Sediments in ppm and Enrichment Factors in Marine Sediments

	EF OZ331	EF OZ332	EF TRE21.5	EF TRE32	EF TRE44	EF TRE72
Na	0.342	0.309	0.458	6.75	0.377	0.306
Mg	1.63	1.36	1.54	6.59	0.709	0.653
Al						
Si	1.01	0.951	0.875	1.47	0.963	0.855
P	2.43	0.756	4.63	17.33	0.778	0.345
K	0.42	0.598	0.3	1.98	0.658	0.721
Sc	1.25	1.47	1.23	2.72	1.14	1.12
Ti	0.896	0.9	0.832	187.28	1.01	0.978
V	1.47	1.34	1.29	1.61	1.04	1.15
Cr	2.21	2.25	1.48	5.09	1.26	1.24
Mn	2.08	1.33	4.4	17.17	0.838	1
Fe	1.02	1.08	1.1	0.748	0.801	0.975
Co	1.04	0.719	0.751	2.5	1.01	0.844
Ni	0.996	1.16	1.04	13.25	1.15	1.231
Cu	0.937	1.17	1.33	76.51	0.727	1.131
Zn	1.57	1.75	1.26	23.55	0.932	1.29
As	1.26	0.517	0.687	30	2.04	0.746
Rb	0.436	0.784	0.24	1.14	0.822	0.962
Sr	7.36	4.97	6.22	96.85	1.77	1.53
Y	1.46	1.39	2.02	8.87	0.728	0.731
Zr	1.06	0.935	0.955	7.01	1	0.908
Nb	0.859	0.865	1.028	157.02	1.12	1.19
Sn	2.87	3.26	3.13	36.43	1.56	1.58
Sb						0.318
Cs	0.266	1.28	0.075	2.39	1.64	1.88
Ba	0.309	0.319	0.279	2.71	0.316	0.325
La	1.61	1.68	1.82	8.56	1.01	1.07
Ce	1.05	1.06	1.08	3.56	0.777	0.772
W	1.25	1.91	1.2	137.7	1.24	0.903
Tl	0.088	0.046		1.57	0.014	
Pb	0.379	0.7	0.293	36.7	0.663	0.744
Bi	3.79	2.65	3.12	143.88	2.87	2.72
U	0.779	0.862	0.83	4.84	0.626	0.59

an EF of 1 with the exception in the uppermost part of the profile. Bi is constantly enriched within the whole profile with a distinct peak in EF again in the "Argovien". Zn is enriched to a certain extent within the lowermost part of the profile as well as in the "Argovien". The few measurements of Sb and Tl indicate depletion of these elements throughout.

DISCUSSION

The fluctuation in concentrations of the main elements like Na, Mg, Al, Si and K are very similar and point to an external source (aeolian and fluvial) of these elements. Moreover, those elements are the main constituents in rocks of terrestrial provenance. Al is the most important element essentially not affected by biological or diagenetic processes in marine environments. Biogenic remnants in marine sediments often contain Si, K, Mg, and Na [21]. The main elements, therefore, are not suitable for the use as palaeoproxies.

By far the most extensively studied trace elements in marine sediments are Fe and Mn (e.g. [4, 7-9, 12, 18, 20, 21, 26, 29, 31, 40-45]). According to Bruland [21] Mn occurs dissolved in the sea in the +2 oxidation state and tends to form relatively weak complexes in seawater mostly like the free hydrated Mn^{2+} or $MnCl^{+}$. In oxygenated seawater Mn(II) is thermodynamically unstable and tends to form insoluble manganese oxides. Mn is mainly delivered to the ocean by external input sources (physical weathering, erosion of rocks, aeolian and fluvial transport) which lead to maxima in the surface waters, in the oxygen-minimum zone. Other mechanisms of Mn input consist of remobilization of Mn from sediments and hydrothermal flux. The high solubility of Mn^{2+} in sediments deposited under reducing conditions may result in Mn being depleted in the sediment if fixation in carbonate minerals does not occur [9]. Mn redox cycling is inasmuch important for trace-metal enrichment in suboxic-anoxic systems because it can trigger and/or accelerate the transfer of trace elements from seawater to the sediment (e.g. adsorption of trace metals onto Mn-oxyhydroxides) as well as the diagenetic remobilization of trace elements within the sediment [e.g. 17, 19].

Fe - the most abundant metal in the Earth's crust - is stable as Fe(III) in oxygenated seawater. Dissolved Fe(III), due to its strong tendency to hydrolyze, exists in seawater mainly as $Fe(OH)_3^0$ and $Fe(OH)^{2+}$. Fe(III) preferably precipitates as hydrous iron oxide. Fe(II) exists as a stable form in anaerobic waters as the free ion or $FeCl^{+}$. Fe features a similar pattern of redox cycling to Mn although with a remarkable difference: Fe is systematically involved in Fe-sulfide precipitation within reducing sediments and waters and is sequestered in Fe-carbonates (i.e., siderite) only under special conditions. The natural input of Fe is dominated by particulate transport from the continents in the form of suspended material in rivers or aeolian dust, input as complexes, colloids and particles < 0.45 µm and hydrothermal flux [8, 21, 31]. The major sink of Fe in the oceanic (hemipelagic and pelagic) environment is the formation of Fe-sulfides in reducing sediments. The most striking feature within the Oxfordian sediments from Trescléoux and Oze concerning Fe and Mn is the correlation of the enrichment of these two elements with the positive $\partial^{13}C$ excursion in the upper part of the profile ("Argovien"). This correlation of the $\partial^{13}C$ excursion with trends in Mn and Fe contents seems to reflect changes in the Oxfordian palaeooceanography and climate. High concentrations of Mn of the early Toarcian, Late Jurassic, Aptian, Albian, Cenomanian/Turonian boundary and Miocene seem to be correlated with ocean-wide anoxia (Oceanic Anoxic Events OAE) and/or changes in the carbon cycle as expressed by positive $\partial^{13}C$ excursions (e.g. [31, 32, 46-49]) within hemipelagic to pelagic environments [1]. The climate during the Oxfordian was undergoing major changes, during this time interval a transition of a cold and humid period to a considerably warmer and more arid climate proceeded. This change led to increased metal flux from the continent due to the intensified chemical weathering, triggered by the onset of intensified greenhouse climate conditions recorded by the perturbation of the C-isotope curve. The turning point of the excursion coincides with a major change in Tethyan sedimentation pattern [1]. According [2] there is no evidence for large-scale volcanism during the Oxfordian.

Other redox-sensitive elements include V, Cr, Co, Ni and U. V is present in oxygenated seawater in +5 oxidation state, mainly as VO_2^{2+} and $HV_2O_4^{-}$. Under anoxic conditions it is reduced to the oxovanadium (IV) ion, VO_2^{2+} [21]. In pelagic and hemipelagic sediments, V is tightly coupled with the redox cycle of Mn [50]. Vanadate readily adsorbs onto both Mn- and Fe-oxyhydroxides [8]. U in seawater is present mainly as U(VI) in the conservative form of uranyl ions that bind to carbonate ions, forming $UO_2(CO)_3^{4-}$.

Reduction of U (VI) to U(IV) occurs under conditions similar to those of Fe(III) to Fe(II) [51-53]. In the reduced state, removal of U from the water column and accumulation into the sediment is at least partly mediated by bacterial sulfate reduction reactions, because without bacterial activity, the reduction process would be very slow [53, 54]. In Tribovillard *et al.* [19] an interesting aspect of the geochemistry of U is pointed out. As the intensity of sulfate reduction activity is linked to the abundance of reactive organic matter (bacteria), U abundance usually shows a good correlation with the organic carbon rain rate and with the organic-carbon content in anoxic (non-sulfidic) facies. Another fact of the geochemistry of V and U deserves mentioning as well: Both elements are reduced and can accumulate under denitrifying conditions, whereas Ni, Co, Cu, Zn, Cd and Mo are enriched mainly under sulfate-reducing (euxinic) conditions alone [8, 15, 18, 23, 25]. Using the contrasting behavior of these two groups of trace elements, it may be possible to recognize redox gradations in some sedimentary systems. For example, in the case of U and V enrichment without Mo enrichment, suboxic/anoxic depositional without free H_2S can be inferred. Conversely, sediments exhibiting concurrent enrichments in U, V and Mo reflect euxinic conditions at the sediment-water interface or in the water column [18, 23, 55, 56].

As Mo and Cd are not detectable (e.g. both elements are well below LOD) in the marine sediments from both Trescléoux and Oze, euxinic conditions at the time of deposition can be excluded. V and U both exhibit the typical peak within positive $\partial^{13}C$ excursion in the upper part of the

profile and this fact can be taken as a good indication for an OAE. V and U both have in common that there is no detrital influence to their concentration in marine sediments. As already mentioned above, the turning point of the isotope excursion coincides with a major change in the Tethyan sedimentation pattern [1-3]. This was also the time of a profound rearrangement of the oceanic current system induced by the establishment of a new circum-global ocean passage in low latitudes. This modification very likely increased temperatures by about 5°C in middle latitudes and increased nutrient concentrations in surface water due to intensified upwelling. The result was an increased C_{org} production and burial, leading to the positive excursion in C-isotope records as ^{12}C was preferentially removed from the ocean system ([1, 2] and references therein).

Cr, Co and Ni represent redox-sensitive trace elements as well and display a similar distribution pattern to U and V but exhibit greater fluctuations within the middle part of the profile. In oxygenated seawater, Cr is present primarily as Cr(VI) in the chromate anion. Under usual seawater conditions, the chromate anion is soluble, but under anoxic conditions, Cr(IV) is reduced to Cr(III), forming aquahydroxyl cations and hydroxyl cations which can readily be adsorbed to Fe- and Mn-oxyhydroxides [8, 21]. Thus, Cr is exported to the sediments. More over, Cr may be transported to the sediment with the land-derived clastic fraction (e.g., chromite, clay minerals, ferromagnesian minerals in which Cr substitutes readily for Mg [6, 9, 57]. Thus, the complexities of Cr transport and enrichment limits its palaeoenvironmental utility.

Co and Ni can both be incorporated into pyrite, the most common sulfide in the marine sediments taken for this study. In oxic environments, Co is present as the dissolved cation, Co^{2+}. In anoxic waters, Co forms the insoluble sulfide CoS, which can be taken up in solid solution by authigenic Fe-sulfides [21]. Co is partially tied to the abundance of clastic material which limits its use as a reliable redox proxy. In oxic marine environments, Ni behaves as a micronutrient and may be present as soluble Ni^{2+} cations or $NiCl^{+}$ ions but it is mostly present as a soluble Ni carbonate ($NiCO_3$) or adsorbed onto humic and fulvic acids [8]. Ni does not show any significant enrichment in the sediments from Trescléoux and Oze, thus again excluding euxinic conditions at the time of deposition.

P is essential to all forms of life on Earth and plays a fundamental role in metabolic processes and is a major constituent of skeletal material. P distributions in sediments are linked to the supply of OM (organic matter), commonly resulting from high productivity [19]. Usually, P is released as PO_4^{3-} from decaying OM during oxic, suboxic and anoxic bacterial degradation below the sediment-water interface. P remineralized to pore waters can either be released from the sediment back to the water column or can be reprecipitated within the sediment (e.g. [58]). Under certain conditions, P once released to pore water can reach relatively high concentrations and authigenic phases can precipitate. The principal authigenic phases belong to the apatite family. A prerequisite for precipitation is supersaturation of P.

High productivity is not always considered necessary for an enrichment of P. In low productivity areas of the oceans, P accumulation can be achieved through redox cycling of Fe, with P sorption onto Fe-oxyhydroxide coatings and Fe-P co-precipitation (e.g. [59]). As mentioned by [60] Mn can also be involved in P enrichment. Thus, in the case of P trapping in sediments, the abundance of P is not necessarily indicative of a high productivity area. P can also be retained as a reactive fraction in the sediments which depend highly on the redox conditions of the depositional system. The elevated concentration in the sediments from Trescléoux and Oze in the "Argovien" (upper positive $\partial^{13}C$ excursion) coincide precisely with the peaks of Fe and Mn. Anoxic conditions are indicated by Fe, Mn and P, although the influence of high productivity cannot be excluded. The high concentration of the nutrient related element P in the lowermost part of the Oze section suggests a more oligotrophic setting with an elevated biological productivity [9, 25]. As the principal authigenic phases belong to the apatite family, many elemental (major and trace elements) substitutions can occur in the two Ca sites as well as in the PO_4 and F site or may be adsorbed onto the crystal surface.

Elements showing marked enrichments within the marine sediments of southern France include Y, the rare earth elements and accessorily Cu, Cr, Pb and V [61]. Sc, Y, La and Ce have very similar chemical and physical properties due to the fact that they all form stable 3^{+} ions of similar size. Ce also exists in the 4^{+} state and, therefore, redox conditions can affect its chemistry. Theoretical considerations suggest that trivalent REE should exhibit strong, predominantly electrostatic complexing with "hard" ligands such as fluoride, sulfate, phosphate, carbonate and hydroxide [62]. Enrichments of the rare earth element Ce incidentally seem to be indicative of anoxic conditions, too. Trends in Ce anomalies may broadly reflect changes in local oxygen availability, but this does not enable them to be used as global surface redox indicator [14]. The REEs are regarded as being almost insoluble and are present in only very low concentrations in seawater [63]. Thus, the REEs present in sediments are mainly transported as particulate matter and reflect the chemistry of their source areas. Although there was considerable research done on REE during the last decade, there is still much debate over the use of REE as palaeoproxies (e.g. [14, 64, 65].

Rb and Sr can easily substitute for K or Ca in their respective mineral phases. For Rb this fact is evident due to the close correlation of the distribution and peak pattern for K and Rb. The latter element substitutes readily for K and is mainly found in the K feldspars and micas - the most prominent detrital minerals in the samples from southern France. The high content of Sr which always shows a strong correlation with Ca (due to its primary fixation in the lattice of calcareous skeletal material) supports the thesis of a more oligotrophic setting (similar to P) within the "Terre Noires". Ce behaves very similar to Rb. Sc is to-date not known to be a palaeoproxy not being subject to chemical and/or physical fractionation and is not preferentially incorporated in any mineral phase.

Certain trace elements can stringently be used as palaeoproxies of detrital origin. One of these elements is Ti, which is overwhelmingly of detrital origin and is usually immobile during diagenesis (see e.g. [8, 9, 15]). In seawater Ti is mainly present as Ti(IV) and the hydrolyzed species is

the main form in aqueous solution. In Bruland [21] the author states that its concentration in seawater must be very low as the readiness with which it hydrolyses implies a very short residence time.

The heavy metals Zr, Nb and W are also of detrital origin. Zr and Nb are often concentrated in heavy-metal mineral associations whereas Ca and Sr reflect the occurrence of carbonate [29]. Enhanced concentrations of Zr and Nb seem to be of volcanogenic origin [21, 25, 26]. This interpretation can be excluded as in Louis-Schmid *et al*. [1] the authors see no evidence for volcanism during the Oxfordian. Ti, Nb and W exhibit a clear increase in concentration again within the upper part of the profile (e.g. the positive $\partial^{13}C$ excursion *senso stricto*). Again, this correlation of the $\partial^{13}C$ excursion with trends in Ti, Nb, and W as well as Mn and Fe contents seems to reflect changes in the Oxfordian palaeooceanography and climate [1-4]. The climate during the late Oxfordian was dominated by warm and arid conditions. Such conditions resulted in an increased metal flux from the continent due to the intensified chemical and physical weathering, erosion of rocks, aeolian and fluvial transport to the oceans at elevated temperatures. Zr shows a rather irregular pattern with regard to concentrations due to sample preparation difficulties concerning this element.

The concentrations of Cu and As are evenly distributed below the $\partial^{13}C$ excursion. The usual spike within the $\partial^{13}C$ excursion is evident. In oxic marine environments, Cu is dominantly present as organometallic ligands and, to a lesser degree, $CuCl^+$ ions present in solution [8, 21]. Copper can behave partly as a micronutrient but can also be scavenged from solution in deep water [8] as well as be adsorbed onto particulate Fe-Mn-oxyhydroxides [66]. Under reducing conditions (notably bacterial sulfate reduction conditions), Cu(II) is reduced to Cu(I) and may be incorporated in solid solution in pyrite, or it may even form its own sulfide phases, CuS and CuS_2 [67, 68]. Therefore, it is not surprising that Cu follows the distribution pattern of Fe with an enrichment in the upper part of the profile. As is similarly distributed to Cu. As described above Cu as well as As can be incorporated in pyrite or may form sulfide phases of their own [69]. Both elements are affected by changing redox conditions and productivity, similarly to V and U [15] and have a nutrient type distribution. According to Warning and Brumsack [70], Bi is often enriched in sapropels. This fact possibly indicates fixation of Bi in anoxic waters and sediments owing to the formation of sulfides - and this is again a good indicator of an OAE.

Zn, Sn and Pb do not display any distinct peak or drop in concentration within the profile. In oxic marine environments Zn behaves as a micronutrient, its distribution highly correlated with that of Si and may be present as soluble Zn^{2+} cations or $ZnCl^+$ ions [8, 16, 18, 21]. Zn is considered to be added to the sediment essentially in association with planktonic materials [6]. High concentrations of Zn in marine sediments are also assigned to hydrothermal input [4, 18, 27, 28]. Zn may also be adsorbed onto particulate Fe-Mn-oxyhydroxides [71]. Under reducing conditions Zn may be incorporated as ZnS as a solid solution phase in pyrite or, to a lesser degree, it may form its own sulfides, mainly sphalerite [67, 68]. Because of this variety of behavior of Zn in the marine environment, it cannot be used as a meaningful palaeoproxy. This is illustrated by the oscillating concentrations without any obvious enrichments or peaks within the profile.

Sn and Pb display a distribution pattern analogous to Zn. Very little is known about the use of the first mentioned elements as palaeoproxies. High concentrations of Pb in marine sediments are often attributed to anthropogenic sources. This influence can obviously be excluded in marine sediments from the Oxfordian. Sn and Pb as well as Si are part of the same group of the periodic table of the elements and exist both in the 2^+ (Sn, Pb) and 4^+ (Si, Sn) oxidation state. In seawater Sn is present in the 4^+ and Pb in the 2^+ state, predominantly as hydroxy- and chloro-complexes. Sn and Pb are involved in biologically mediated reactions [21]. In seawater Pb has a low abundance, a very short residence time, and is rapidly scavenged. Marine plankton exhibits elevated contents of Pb. In pre-historic marine sediments Pb is not enriched above their lithogenic background [72].

Sb and Tl are mainly enriched in sediments formed under euxinic conditions [72] and these specific conditions can be excluded as explained above. Therefore only a few statistically relevant measurements could be performed as the concentration of Sb and Tl in the marine sediments from Trescléoux and Oze is very low.

Ba concentrations fluctuate within the lower part of the profile and increase steadily to values up to 600 ppm within the middle before dropping again. No distinct peak within the $\partial^{13}C$ excursion can be seen. Ba is occasionally of detrital provenance but is mainly present in marine sediments in detrital plagioclase crystals and as barite ($BaSO_4$) ([19] and references therein). Phytoplankton incorporate Ba and the element is released during phytoplanktonic decay and may later precipitate as barite in micro-environments where Ba-sulfate reaches supersaturation (e.g. [73]). The apparent association of biogenic barite and OM have given support to the idea of using Ba as proxy for palaeoproductivity (e.g. [73, 74]).

Many research works have dealt with the concept of using biogenic Ba as a palaeoproductivity proxy in older sediments (see [19] and references therein). But this approach should be used cautiously as in the case of sediments characterized by intense sulfate reduction, barite dissolution and Ba migration can occur (see [19] and references therein). Therefore, it is plausible that Ba enrichment in sediments is coupled to a high OM flux but can migrate during early diagenesis and precipitate in sediments formed under low productivity conditions. The indicated sulfate-reducing conditions can develop rapidly in OM-rich sediments - this fact is convincing enough to state that Ba abundance cannot be used confidently as an indicator of an enhanced palaeoproductivity in organic-rich sediments. The effectiveness of the use of the Ba palaeoproductivity marker may be restricted to marine sediments deposited in portions of the ocean with low to moderate productivity [19]. Similar to P the influence of a high productivity area cannot be excluded. Low to moderate productivity seems more convincing as the Ba concentration is fluctuating constantly within the whole profile. A peak in concentration appears well below the uppermost positive $\partial^{13}C$ excursion (not shown in Fig. **3**).

U exhibits an identical peak at the same location as well: Sulfate reduction by organic matter (important for the U abundance in sediments usually exhibiting a good correlation with the organic-carbon content in anoxic (non-sulfidic facies) promotes enrichment of U in sediments. Ba enrichment is well known to be linked to high OM flux. There is a steady increase in concentration of Ba in the sediments from Oze peaking within sample OZ300 and an immediate drop thereafter. The drop in concentration in U is of the same type. The gradual, steady increase of Ba suggests a slow response of the environmental system to enhanced sulfate reduction by organic matter peaking in sample OZ300 and the sudden decline in the concentration of Ba as sulfate is consumed. As Ba can migrate during early diagenesis and precipitate in sediments formed under low productivity, the interpretation of a low productivity area in the middle part of the profile seems correct.

The inspection of the enrichment factors EF regarding the element/Al ratios of average shale compared to marine sediments substantiates the interpretation of enrichments of certain elements used as palaeoproxies for the terrigenous-detrital fraction in marine sediments: P, Ti, Mn, Fe, Sr, Y, Zr, Nb, La, Ce, W, Pb and including Sc are highly enriched compared to Al in the average shale in the uppermost part of the profile ("Argovien"). All these elements are largely transported to the ocean by external sources. The climate during the Oxfordian was undergoing major changes with a transition of a cold and humid period to a considerably warmer and more arid climate. This change led to increased metal flux from the continent due to the intensified chemical weathering. The turning point of the excursion coincides with a major change in Tethyan sedimentation pattern [1, 2].

V, Co and Ni never show a distinct enrichment except within the uppermost part of the profile. These elements are all redox-sensitive and are not part of the detrital fraction. Cr often exhibits enrichment factors around 2 and again a peak in EF in the "Argovien" section. Cr may be transported to the sediment with the land-derived clastic fraction but is also an indicator of anoxic environmental conditions. Cu and As commonly oscillate around an EF of 1 except in the uppermost part of the profile. Bi is constantly enriched within the whole profile with a distinct peak in EF again in the "Argovien". This again points to anoxic conditions. The few measurements of Sb and Tl indicate depletion of these elements throughout. They are both tracers for euxinic conditions and this specific environment can be excluded as explained above.

SUMMARY AND CONCLUSIONS

Certain trace elements can be used as palaeoproxies as discussed above. As the climate was undergoing major changes during the Oxfordian, the cold and humid period of the late Callovian-early Oxfordian gave way to a warmer and more arid climate in the middle-late Oxfordian. Along with the ongoing opening of the Atlantic and the Tethys, the Late Jurassic long-term sea-level rise led to a reorganization of ocean currents in the Tethys-Atlantic system during the Oxfordian. Together with the carbon isotope records of marine carbonate used as a proxy of the carbon cycle the following pattern of the above described changes could be established.

During the deposition of the so called "Terre Noires" at Trescléoux and Oze (grey to black marls, which contain layers of carbonate nodules parallel to the bedding) the high concentrations of P and Sr point to a more oligotrophic setting as P can be readily sorbed onto Fe and Mn-oxyhydroxide coatings. This is in accordance with the high Mn and Fe concentrations in the marine sediments from these two localities. The high content of Sr, which always shows a strong correlation with Ca, enhances the thesis of a more oligotrophic setting (similar to P) within the "Terre Noires", too. Barium enrichment in sediments is coupled to a high OM flux but Ba can migrate during early diagenesis and precipitate in sediments formed under low productivity conditions.

The high concentration peaks of P in the sediments of Oze and Trescléoux in the "Argovien" (upper positive $\partial^{13}C$ excursion with $\partial^{13}C$ values rising from 2 to 3 ‰) coincide precisely with the peaks of Fe and Mn. Anoxic conditions are indicated by Mn, Fe and P although an influence of a high productivity area concerning the P concentration cannot be excluded. Another stringent argument for an ocean-wide anoxia consists of the enrichment of the redox-sensitive elements V and U. The latter elements are in their reduced state and can accumulate under denitrifying or anoxic conditions, whereas Ni, Co, Cu, Zn, Cd and Mo are enriched mainly under sulfate-reducing (euxinic) conditions alone. As Mo and Cd are not detectable, euxinic conditions at the time of deposition can be excluded. The low concentrations of Sb and Tl exclude euxinic conditions, as well.

High detrital input during the period of the upper positive $\partial^{13}C$ excursion is recorded by enhanced concentrations of elements like Ti, Mn, Fe, Zr, Nb and W. Tit, Zr, Nb and W are incorporated in heavy minerals and are usually immobile during diagenesis. This correlation of the $\partial^{13}C$ excursion with trends in Ti, Nb, W as well as Mn and Fe contents seems to reflect changes in the Oxfordian palaeooceanography and climate as during the late Oxfordian the environmental prerequisites were controlled by warm and arid conditions and an increased metal flux from the continent due to the intensified chemical and physical weathering, erosion of rocks, aeolian and fluvial transport to the oceans.

(1) The concentration patterns of P, Sr, Mn, Fe and Ba point to an oligotrophic setting within the sediments belonging to the "Terre Noires" facies.

(2) An ocean-wide anoxia event within the Tethys is detected by the significant enrichment of P, V, Mn, Fe and U which coincides with $\partial^{13}C$ excursion of the "Argovien" facies. Due to the low abundances of Co, Ni, Cu, and Zn and the absence of Mo, Cd, Sb and Tl euxinic conditions can be excluded.

(3) High detrital input during the period of the upper positive $\partial^{13}C$ excursion as well as warm and arid conditions is proved by enhanced concentrations of the elements Ti, Mn, Fe, Zr, Nb and W.

ACKNOWLEDGEMENTS

Thanks go to Beat Louis-Schmid for collecting and providing the samples from Trescléoux and Oze, Marcel Guillong for the LA-ICP-MS analyses, Lydia Zehnder for

the XRF measurements, Helmut Weissert for the scientific input and Terry Seward for the linguistic revision. The long term support from Geneviève Défago and Günter Kahr at the ETH Zürich is also acknowledged with thanks.

CONFLICT OF INTEREST

The author confirms that this article content has no conflict of interest.

REFERENCES

[1] Louis-Schmid B, Rais P, Bernasconi SM, Pellenard P, Collin PY, Weissert HJ. Detailed record of the mid-Oxfordian (Late- Jurassic) positive carbon-isotope excursion in two hemipelagic sections (France and Switzerland): A plate tectonic trigger? Palaeogeogr Palaeoclimatol Palaeoecol 2007; 248: 459-72.

[2] Louis-Schmid B, Rais P, Schaeffer P, Bernasconi SM, Weissert HJ. Plate tectonic trigger of changes in pCO_2 and climate in the Oxfordian (Late Jurassic): Carbon isotope and modeling evidence. Earth Planet Sci Lett 2007; 258: 44-60.

[3] Louis-Schmid B, Rais P, Logvinovich D, Bernasconi SM, Weissert HJ. Impact of methane seeps on the local carbon-isotope record: a case study from a Late Jurassic hemipelagic section. Terr Nova 2007; 19: 259-65.

[4] Schnetger B, Brumsack HJ, Schale H, Hinrichs J, Dittert L. Geochemical characteristics of deep-sea sediments from the Arabian Sea: a high-resolution study. Deep Sea Res Part II Top Stud Oceangr 2000; 47: 2735-68.

[5] Goldberg ED, Arrhenius GOD. Chemistry of pelagic sediments. Geochim Cosmochim Acta 1958; 29: 153-212.

[6] François R. A study on the regulation of the concentration of some trace elements (Rb, Sr, Zn, Pb, Cu, V, Cr, Ni, Mn and Mo) in Saanich Inlet sediments, British Columbia, Canada. Mar Geol 1988; 83: 285-308.

[7] Shaw TJ, Gieskesm JM, Jahnke RA. Early diagenesis in differing depositional environments: The response of transition metals in pore water. Geochim Cosmochim Acta 1990; 54: 1233-46.

[8] Calvert SE, Pedersen TF. Geochemistry of recent oxic and anoxic marine sediments: implications for the geological record. Mar Geol 1993; 113: 67-88.

[9] Hild A, Brumsack HJ. Major and minor element geochemistry of lower Aptian sediments from the NW German Basin (core Hohenegglesen KB 40). Cretaceous Res 1998; 19: 615-33.

[10] Brumsack HJ, Wehausen R. A. Geochemical record of precession-induced cyclic Eastern Mediterranean sedimentation: Implications for Northern Sahara humidity during the Pliocene. Naturwissenschaften 1999; 86: 281-6.

[11] Morford JL, Emerson S. The geochemistry of redox sensitive trace metals in sediments. Geochim Cosmochim Acta 1999; 63: 1735-50.

[12] Wehausen R, Brumsack HJ. Cyclic variations in the chemical composition of eastern Mediterranean Pliocene sediments: a key for understanding sapropel formation. Mar Geol 1999; 153: 161-76.

[13] Dellwig O, Watermann F, Brumsack HJ, Gerdes G, Krumbein WE. Sulphur and iron geochemistry of Holocene coastal peats (NW Germany): a tool for palaeoenvironmental reconstruction. Palaeogeogr Palaeoclimatol Palaeoecol 2001; 167: 359-79.

[14] Shields G, Stille P. Diagenetic constraints on the use of cerium anomalies as palaeoseawater redox proxies: an isotopic and REE study of Cambrian phosphorites. Chem Geol 2001; 175: 29-48.

[15] Böning P, Brumsack HJ, Böttcher ME, *et al*. Geochemistry of Peruvian near-surface sediments. Geochim Cosmochim Acta 2004; 68: 4429-51.

[16] Babu CP, Brumsack HJ, Schnetger B, Böttcher ME. Barium as a productivity proxy in continental margin sediments: a study from the eastern Arabian Sea. Mar Geol 2002; 184: 189-206.

[17] Morford JL, Emerson SR, Breckel EJ, Kim SH. Diagenesis of oxyanions (V, U, Re, and Mo) in pore waters and sediments from a continental margin. Geochim Cosmochim Acta 2005; 69: 5021-32.

[18] Brumsack HJ. The trace metal content of recent organic carbon-rich sediments: Implications for Cretaceous black shale formation. Palaeogeogr Palaeoclimatol Palaeoecol 2006; 232: 344-61.

[19] Tribovillard N, Algeo TJ, Lyons T, Riboulleau A. Trace metals as palaeoredox and palaeoproductivity proxies: An update. Chem Geol 2006; 232: 12-32.

[20] Beck M, Dellwig O, Schnetger B, Brumsack HJ. Cycling of trace metals (Mn, Fe, Mo, U, V, Cr) in deep pore waters of interdital flat sediments. Geochim Cosmochim Acta 2008; 72: 2822-40.

[21] Bruland KW. Trace elements in seawater. Chem Oceanogr 1983; 8: 157-220.

[22] Craig PJ, Miller D. Metal ions and organometallic compounds in sea water and in sediments: biogeochemical cycles. In: Gianguzza A, Pelizzetti E, Sammartano S, Eds. Marine Chemisty. Dordrech: Kluwer Academic Publishers 1997; pp. 85-97.

[23] Rinna J, Warning B, Meyers PA, Brumsack HJ, Rullkötter J. Combined organic and inorganic geochemical reconstruction of palaeodepositional conditions of a Pliocene sapropel from the eastern Mediterranean Sea. Geochim Cosmochim Acta 2002; 66: 1969-86.

[24] Goldschmidt VM. Geochemistry. In: Muir A, Ed. The International Series of Monographs on Physics. Oxford: Clarendon Press 1954.

[25] Brumsack HJ. The inorganic geochemistry of Cretaceous black shales (DSDP Leg 41) in comparison to modern upwelling sediments from the Gulf of California. In: Summerhayes CP, Shakleton NJ, Eds. North Atlantic Palaeoceanography. London, UK: Geological Society Special Publication 1986; vol. 21: pp. 447-62.

[26] Rachold V, Brumsack HJ. Inorganic geochemistry of Albian sediments from the Lower Saxony Basin NW, Germany: palaeoenvironmental constraints and orbital cycles. Palaeogeogr Palaeoclimatol Palaeoecol 2001; 174: 121-43.

[27] Bruland KW. Oceanographic distributions of cadmium, zinc, nickel, and copper in the north pacific. Earth Planet Sci Lett 1980; 47: 176-98.

[28] Lipinski M, Warning B, Brumsack HJ. Trace metal signatures of Jurassic/Cretaceous black shales from the Norwegian Shelf and the Barents Sea. Palaeogeogr Palaeoclimatol Palaeoecol 2003; 190: 459-75.

[29] Dellwig O, Hinrichs J, Hild A, Brumsack HJ. Changing sedimentation in tidal flat sediments of the southern North Sea from the Holocene to the present: a geochemical approach. J Sea Res 2000; 44: 195-208.

[30] Müller B. Impact of the bacterium *Pseudomonas fluorescens* and its genetic derivatives on vermiculite: Effects on trace metals contents and clay mineralogical properties. Geoderma 2009; 153: 94-103.

[31] Kuhn O, Weissert HJ, Föllmi KB, Henning S. Altered carbon cycling and trace-metal enrichment during the late Valanginian and early Hauterivian. Eclogae Geol Helv 2005; 98: 333-44.

[32] Schlanger SO, Arthur MA, Jenkyns HC, Scholle PA. The Cenomanian-Turonian anoxic event, 1. stratigraphy and distribution of organic carbon rich beds and the marine $\partial^{13}C$ excursions. In: Brooks J, Fleet AJ, Eds. Marine Petroleum Source Rocks. London, UK: Geological Society Special Publications 1987; vol. 26: pp. 371-99.

[33] Bodin S, Godet A, Matera V, *et al*. Enrichment of redox-sensitive trace metals (U, V, Mo, As) associated with the late Hauterivian Faraoni oceanic anoxic event. Int J Earth Sci (Geologische Rundschau) 2006; 96: 327-41.

[34] Westermann S, Föllmi KB, Adatte T, *et al*. The Valanginian $\delta^{13}C$ excursion may not be an expression of a global oceanic anoxic event. Earth Planet Sci Lett 2010; 290: 118-31.

[35] Günther D, Frischknecht R, Heinrich CA, Kahlert HJ. Capabilities of an argon fluoride 193 nm excimer laser for laser ablation inductively coupled plasma mass spectrometry microanalysis of geological materials. J Anal At Spectrom 1997; 12: 939-44.

[36] Pettke T, Audétat A, Schaltegger U, Heinrich CA. Magmatic-to-hydrothermal crystallization in the W-Sn mineralized Mole Granite (NSW, Australia). Chem Geol 2005; 220: 191-213.

[37] Longerich HP, Jackson SE, Günther D. Laser ablation inductively coupled plasma mass spectrometric transient signal data acquisition and analyte concentration calculation. J Anal At Spectrom 1996; 11: 899-904.

[38] Heinrich CA, Pettke T, Halter WE, *et al*. Quantitative multi-element analysis of minerals, fluid and melt inclusions by laser-ablation inductively-coupled mass-spectrometry. Geochim Cosmochim Acta 2003; 67: 3473-97.

[39] Müller B, Guillong M. Laser Ablation ICP-MS analyses of marine sediments from the Oxfordian (Late Jurassic): A comparison of three preparation techniques. Open Miner J 2010; 4: 9-19.

[40] Bender ML, Klinkhammer GP, Spencer DW. Manganese in seawater and the marine manganese balance. Deep-Sea Res 1977; 24: 799-812.

[41] Tebo BM, Rosson RA, Nealson KH. Potential for manganese(II) oxidation and manganese (IV) reduction to co-occur in the suboxic

zone of the black sea. In: Izdar E, Murray JW, Eds. Black Sea Oceanography. USA: Kluwer Academic Publishers 1986; pp. 173-85.
[42] Calvert SE, Bustin RM, Ingall ED. Influence of water column anoxia and sediment supply on the burial and preservation of organic carbon in marine shales. Geochim Cosmochim Acta 1996; 60: 1577-93.
[43] Dellwig O, Watermann F, Brumsack HJ, Gerdes G. High-resolution reconstruction of a Holocene coastal sequence (NW Germany) using inorganic geochemical data and diatom inventories. Estuar Coast Shelf Sci 1999; 48: 617-33.
[44] Böning P, Cuypers S, Grunwald M, Schnetger B, Brumsack HJ. Geochemical characteristics of Chilean upwelling sediments at ~36°S. Mar Geol 2005; 220: 1-21.
[45] Collin PY, Loreau JP, Courville P. Depositional environments and iron ooid formation in condensed sections (Callovian-Oxfordian, south-eastern Paris basin, France). Sedimentology 2005; 52: 969-85.
[46] Weissert HJ. C-Isotope stratigraphy, a monitor of palaeoenvironmental change: a case study from the Early Cretaceous. Surv Geophys 1989; 10: 1-61.
[47] Weissert HJ, Lini A, Föllmi KB, Kuhn O. Correlation of Early Cretaceous carbon isotope stratigraphy and platform drowning events: a possible link. Palaeogeogr Palaeoclimatol Palaeoecol 1998; 137: 189-203.
[48] Kump LR, Arthur MA. Interpreting carbon-isotope excursions: carbonates and organic matter. Chem Geol 1999; 161: 181-98.
[49] Erba E, Bartolini A, Larson RL. Valanginian Weissert oceanic anoxic event. Geology 2004; 32: 149-52.
[50] Hastings DW, Emerson SR, Mix AC. Vanadium in foraminiferal calcite as a tracer for changes in the areal extent of reducing sediments. Palaeoceanography 1996; 11: 665-78.
[51] Zheng Y, Anderson RF, van Geen A, Kuwabara J. Authigenic molybdenum formation in marine sediments: a link to pore water sulfide in the Santa Barbara Basin. Geochim Cosmochim Acta 2000; 64: 4165-78.
[52] Morford JL, Russell AD, Emerson S. Trace metal evidence for changes in the redox environment associated with the transition from terrigenous clay to diatomaceous sediments, Saanich Inlet, BC. Mar Geol 2001; 174: 355-69.
[53] McManus J, Berelson WM, Klinkhammer GP, Hammond DE, Holm C. Authigenic uranium: relationship to oxygen penetration depth and organic carbon rain. Geochim Cosmochim Acta 2005; 69: 95-108.
[54] Zheng Y, Anderson RF, van Geen A, Fleisher MQ. Remobilization of authigenic uranium in marine sediments by bioturbation. Geochim Cosmochim Acta 2002; 66: 1759-72.
[55] Tribovillard N, Riboulleau A, Lyons T, Baudin F. Enhanced trapping of molybdenum by sulfurized organic matter of marine origin as recorded by various Mesozoic formations. Chem Geol 2004; 213: 385-401.
[56] Tribovillard N, Ramdani A, Trentesaux A. Controls on organic accumulation in Late Jurassic shales of northwestern Europe as inferred from trace-metal geochemistry. In: Harris N, Ed. The Deposition of Organic-Carbon-Rich Sediments: Models, Mechanisms, and Consequences. Tulsa: SEPM Special Publication 2005; 82: pp. 145-64.
[57] Brumsack HJ. Geochemistry of recent TOC-rich sediments from the Gulf of California and the Black Sea. Geol Rundsch 1989; 78: 851-82.
[58] Kidder DL, Krishnaswamy R, Mapes RH. Elemental mobility in phosphatic shales during concretion growth and implications for provenance analysis. Chem Geol 2003; 198: 335-53.
[59] Piper DZ, Perkins RB. A modern *vs* Permian black shale - the hydrography, primary productivity, and water-column chemistry of deposition. Chem Geol 2004; 206: 177-97.
[60] Wang Y, van Cappellen P. A. multicomponent reactive transport model of early diagenesis: application to redox cycling in coastal marine sediments. Geochim Cosmochim Acta 1996; 60: 2993-3014.
[61] Jarvis I, Burnett WC, Nathan Y, *et al*. Phosphorite geochemistry: state of the art and environmental concerns. Eclogae Geol Helv 1994; 87: 643-700.
[62] Wood SA. The aqueous geochemistry of the rare-earth elements and yttrium: 1. Review of available low-temperature data for inorganic complexes and the inorganic REE speciation of natural waters. Chem Geol 1990; 82: 159-86.
[63] McLennan SM. Rare earth elements in sedimentary rocks: influence of provenance and sedimentary processes. In: Lipin BR, McKay GA, Eds. Geochemistry and Mineralogy of the Rare Earth Elements. USA: Minerological Soc Am 1989; vol. 21: pp. 169-200.
[64] Hetzel A, Brumsack HJ, Schnetger B, Böttchers ME. 8. Inorganic geochemical characterization of lithologic units recovered during ODP LEG 207 (Demerata Rise). In: Mosher DC, Erbacher J, Malone MJ, Eds. Proceedings of the Ocean Drilling Program, Scientific Results. USA: College Station 2006; vol. 207, p. 37.
[65] Al-Mikhlafi AS. Rare earth elements in modern coral sands: an environmental proxy. Environ Geol 2008; 54: 1145-53.
[66] Nameroff TJ, Calvert SE, Murray JW. Glacial-interglacial variability in the eastern tropical North Pacific oxygen minimum zone recorded by redox-sensitive trace metals. Palaeoceanography 2004; 19: PA1010.
[67] Huerta-Diaz MA, Morse JW. Pyritization of trace metals in anoxic marine sediments. Geochim Cosmochim Acta 1992; 56: 2681-702.
[68] Morse JW, Luther III GW. Chemical influences on trace metal-sulfide interactions in anoxic sediments. Geochim Cosmochim Acta 1999; 63: 3373-8.
[69] Sternbeck J, Sohlenius G, Hallberg RO. Sedimentary race elements as proxies to depositional changes induced by a Holocene fresh-brackish water transition. Aquat Geochem 2000; 6: 325-45.
[70] Warning B, Brumsack HJ. Trace metal signatures of eastern Mediterranean sapropels. Palaeogeogr Palaeoclimatol Palaeoecol 2000; 158: 293-309.
[71] Fernex F, Février G, Benaïm J, Arnoux A. Copper, lead and zinc trapping in Mediterranean deep-sea sediments: probable coprecipitation with manganese and iron. Chem Geol 1992; 98: 293-308.
[72] Böning P, Brumsack HJ, Schnetger B, Grunwald M. Trace element signatures of Chilean upwelling sediments at ~36°S. Mar Geol 2009; 259: 112-21.
[73] Dymond J, Suess E, Lyle M. Barium in deep-sea sediments: a geochemical proxy for palaeoproductivity. Palaeoceanography 1992; 7: 163-81.
[74] McManus J, Berelson WM, Hammond DE, Klinkhammer GP. Barium cycling in the North Pacific: implication for the utility of Ba as a palaeoproductivity and palaeoalkalinity proxy. Palaeoceanography 1999; 14: 62-73.
[75] Wedepohl KH. Environmental influences on the chemical composition of shales and clays. In: Ahrens LH, Press F, Runcorn SK, Urey HC, Eds. Physics and Chemistry of the Earth. Oxford: Pergamon 1971; vol. 8, pp. 371-99.
[76] Wedepohl KH. The composition of the upper earth's crust and the natural cycles of selected metals. Metals in natural raw materials. Natural Resources. In: Merian E, Ed. Metals and their Compounds in the Environment. Weinheim: VCH 1991; pp. 3-17.
[77] Ziegler PA. Evolution of the Arctic-North Atlantic and the Western Tethys. Am Assoc Pet Geol Mem 1988; 43: 198.

Received: July 10, 2012 Revised: August 8, 2012 Accepted: August 10, 2012